nature ecology & evolution

SUPPLEMENTARY INFORMATION

https://doi.org/10.1038/s41559-018-0676-2

In the format provided by the authors and unedited.

Demosponge steroid biomarker 26-methylstigmastane provides evidence for Neoproterozoic animals

J. Alex Zumberge[1], Gordon D. Love[1]*, Paco Cárdenas[2], Erik A. Sperling[3], Sunithi Gunasekera[2], Megan Rohrssen[4], Emmanuelle Grosjean[5], John P. Grotzinger[6] and Roger E. Summons[7]

[1]Department of Earth Sciences, University of California, Riverside, Riverside, CA, USA. [2]Department of Medicinal Chemistry, Uppsala University, Uppsala, Sweden. [3]Department of Geological Sciences, Stanford University, Stanford, CA, USA. [4]Department of Earth and Atmospheric Sciences, Central Michigan University, Mount Pleasant, MI, USA. [5]Geoscience Australia, Canberra, Australian Capital Territory, Australia. [6]Division of Geological and Planetary Sciences, California Institute of Technology, Pasadena, CA, USA. [7]Department of Earth, Atmospheric, and Planetary Sciences, Massachusetts Institute of Technology, Cambridge, MA, USA. *e-mail: glove@ucr.edu

Demosponge steroid biomarker 26-methylstigmastane provides evidence for Neoproterozoic animals

Supplementary Information

J. Alex Zumberge[1], Gordon D. Love[1*], Paco Cárdenas[2], Erik A. Sperling[3], Sunithi Gunasekera[2], Megan Rohrssen[4], Emmanuelle Grosjean[5], John P. Grotzinger[6], Roger E. Summons[7]

[1]*Department of Earth Sciences, University of California, Riverside, CA 92521, USA*
[2]*Department of Medicinal Chemistry, Uppsala University, Uppsala 75123, Sweden*
[3]*Department of Geological Sciences, Stanford University, Stanford, CA 94305, USA*
[4]*Department of Earth and Atmospheric Sciences, Central Michigan University, MI 48859, USA*
[5]*Geoscience Australia, Canberra, ACT 2601, Australia*
[6]*Division of Geological and Planetary Sciences, California Institute of Technology, Pasadena, CA 91125, USA*
[7]*Department of Earth, Atmospheric, and Planetary Sciences, Massachusetts Institute of Technology, Cambridge, MA 02139, USA*
*corresponding author: E-mail: glove@ucr.edu; Telephone: 951-827-3181

Contents

1. Overview

Here we report the structure, abundance and temporal range of a new fossil C_{30} sterane for demosponges, 26-methylstigmastane (26-mes, structure **A10** in Chart I) which we have detected in the Neoproterozoic-Cambrian geological record. We quantified the relative and absolute abundances of the 26-mes sterane isomers and we have used the stratigraphic and temporal ranges to constrain the timing of the radiation of sponges (Porifera) within the Neoproterozoic era. We found that 26-mes co-occurs with the previously reported C_{30} sterane biomarker, 24-isopropylcholestane (24-ipc, structure **A5**)[S1] in numerous Cryogenian-Cambrian rock extracts, kerogen hydropyrolysates and oils from the South Oman Salt Basin (SOSB), Eastern Siberia and India (Supplementary Tables 1-3). The record of both 26-mes and 24-ipc steranes commences in Cryogenian-aged sedimentary rocks of the Huqf Supergroup of the South Oman Salt Basin (Ghadir Manquil Formation, ca. 717-635 Myr; and more likely better constrained from Sturtian termination dates as between ca. 660 and 635 Myr, see Fig. 3) and is apparently continuous into the Early Cambrian. While a zircon age of 645 Myr reported from Lahan-1 core from dropstone-bearing siltstones does not help refine our oldest depositional age, since zircons were recovered from just 9 m below the cap dolostone and are likely associated with the top of the Marinoan diamictite, it does support the assignment of the cap dolostone in SOSB strata as being Marinoan in age[S1]. Furthermore, these zircons were isolated from a different drill core to our two interglacial biomarker samples so the relative stratigraphic positions of these to the zircons is uncertain. The Ghadir Manquil Fm. sediment from GM-1 core was a lime mudstone found approximately 150 meters below the base of a diamictite that we interpret as Marinoan age because of the stratigraphic position directly beneath both the Nafun Gp. sedimentary package and the underlying (Marinoan) cap carbonate. The MQR-1 sedimentary rock was a siltstone/sandstone also found below the same sedimentary units in this well. The most parsimonious interpretation in our view then is that Metazoa first achieved ecological prominence in Neoproterozoic marine paleoenvironments most likely between 660 and 635 Myr.

The efficacy of the established 24-ipc sterane record for preserving chemical biosignatures of true sponges has been questioned[S2,S3] since the corresponding sterol precursors, 24-isopropylcholesterol (**B5**) and related structures, have been found in trace amounts in some extant pelagophyte algae. Thus, 24-ipc is not a strictly specific marker for demosponges although this was recognized and reported previously[S1,S4]. Recent molecular clock evidence using gene sequences that encode for sterol methyltransferase (SMT) enzymes (the enzymes that add extra carbon substituents to the sidechains of steroids at the C-24 position) indicates that the pelagophyte algal class diverged much later than the Neoproterozoic era; probably hundreds of millions of years later during the middle Palaeozoic era[S5] (ca. 400 Myr). Thus, it is much less likely that algae were the source of any of the C_{30} steranes in Neoproterozoic rocks, since pelagophytes are the only algal class that make C_{30} regular (4-desmethyl) steranes. Hence, a main conclusion of this published work was that demosponges were the most likely Neoproterozoic source biota for 24-ipc steranes[S5]. Despite this independent support for 24-ipc as a likely Neoproterozoic sponge marker, the caveats have complicated the issue. Our new finding, however, of an additional distinctive ancient sterane biomarker (in the form of 26-mes) adds considerable weight and confidence to the original view that these C_{30} sterane compounds are fossil biomolecules from demosponges and provides a more robust argument for the occurrence of Neoproterozoic Metazoa. While we were cognizant of an unknown series of additional and resolvable peaks in C_{30} sterane ion chromatograms in our original study[S1], we could not at that time positively assign these to specific structures. These mystery peaks have now been unambiguously identified here as diastereoisomers of a single sterane compound series (26-mes), which is an exclusive sterane marker for demosponges (Supplementary Tables 4-5).

The 26-mes sterane series is found in the same Neoproterozoic-Cambrian rock extracts and kerogen pyrolysates from South Oman reported previously[S1,S6], including in two sedimentary rock samples from different cores deposited in the Cryogenian interglacial period (Supplementary Tables 1 & 2 contain original data from Love *et al*., 2009[S1]; but now also with 26-mes sterane data added) below the Marinoan diamictite and cap carbonate. We also detected significant amounts of 26-mes steranes in other Neoproterozoic-Cambrian

rocks and oils that also contain the 24-ipc steranes (Supplementary Table 3). This dual (26-mes and 24-ipc) sterane biomarker record constitutes the oldest current fossil evidence for animals.

2. Huqf Supergroup, South Oman Salt Basin

The Huqf Supergroup provides one of the best preserved, most continuous successions of late Neoproterozoic through earliest Cambrian strata (ca. 713-540 Myr) within subsurface sedimentary basins of the South Oman Salt Basin (SOSB). A description of the geological settings and the different formations, with radiometric age constraints, have been described in detail previously[S1,S6].

Petroleum exploration and production activities of Petroleum Development of Oman allowed us to access numerous deep (1-5 km) sediment cores and cuttings through the Huqf Supergroup as well as oils produced from these thermally well-preserved sediments. The sediments deposited within the Ara Group are commonly called *intra-salt* rocks, whereas rocks deposited before, including those of the Nafun Group, are referred to as *pre-salt* rocks. Ara source rocks deposited in the Athel Basin are commonly referred to as *Athel intra-salt* rocks, as opposed to the Ara carbonate stringers.

64 SOSB source rocks were acquired in total (Supplementary Tables 1-2) and were selected to provide extensive stratigraphic coverage of all formations of the Huqf Supergroup in SOSB. Most of the samples were cutting composites in order to more completely characterize the geochemistry of source rock intervals but some core material was also used. Rocks analyzed had total organic contents (TOCs) of 0.2 to 11 wt.% and the sedimentary organic matter was thermally well preserved, with Hydrogen Indices (HIs) measured from Rock-Eval pyrolysis in the range of 250-700 mg/g TOC[S6]. These HI values are typical of marginal- to middle-oil window source rock maturity and SOSB rocks represent amongst the least thermally altered Neoproterozoic-Cambrian age sediments used to date for molecular biomarker work[S6].

EXPERIMENTAL

3. Catalytic hydropyrolysis of sponge biomass

Continuous-flow hydropyrolysis (HyPy) experiments were performed on 30-150 mg of catalyst-loaded sponge biomass as described previously[S1,S7]. Freeze-dried sponge biomass was initially impregnated with an aqueous methanol solution of ammonium dioxydithiomolybdate [$(NH_4)_2MoO_2S_2$] to give a give a nominal loading of 3-10 wt.% catalyst. Ammonium dioxydithiomolybdate reductively decomposes *in situ* under HyPy conditions above 250ºC to form a catalytically-active molybdenum sulfide (MoS_2) phase.

The catalyst-loaded samples were heated in a stainless steel (316 grade) reactor tube from ambient temperature to 250ºC at 100ºC min^{-1} then to 460ºC at 8ºC min^{-1}. A hydrogen sweep gas flow rate of 6 dm^3 min^{-1}, measured at ambient temperature and pressure, through the reactor bed ensured that the residence times of volatiles generated was the order of only a few seconds. Products were collected on a silica gel trap cooled with dry ice and recovered for subsequent fractionation using silica gel adsorption chromatography.

HyPy products (hydropyrolysates) of sponge biomass were separated by silica gel adsorption chromatography into aliphatic, aromatic and polar (or N, S, O) compounds by elution with *n*-hexane, *n*-hexane:dichloromethane (1:1 v/v) and dichloromethane:methanol (3:1 v/v), respectively. For hydropyrolysates, solvent-extracted activated copper turnings were added to concentrated solutions of aliphatic hydrocarbon fractions to remove all traces of elemental sulfur, which is formed from disproportionation of the catalyst during HyPy. Aliphatic fractions were further purified to a saturated hydrocarbon fraction by the removal of any unsaturated products (alkenes) via silver nitrate impregnated silica gel adsorption chromatography and elution with *n*-hexane.

4. Biomarker analyses

4.1 Analysis of ancient rocks/oils

Detailed methods for extraction and analysis of sedimentary rocks and oils at UCR were described previously[S8-S10] and data is shown in Supplementary Table 3. Rock pieces

were first trimmed with a water-cooled rock saw to remove outer weathered surfaces (at least a few mm thickness) and to expose a solid inner portion and sonicated in a sequence of ultrapure water, methanol, dichloromethane (DCM), and hexane before a final rinse with DCM prior to powdering and bitumen extraction. Rock fragments were powdered in a zirconia ceramic puck mill in a SPEX 8515 Shatterbox, cleaned between samples by powdering two batches of fired sand (850^{o}C overnight) and rinsing with the above series of solvents. Typically, 5 g of crushed rock was extracted in a CEM Microwave Accelerated Reaction System (MARS) at 100°C in a DCM:methanol (9:1 v/v) mixture for 15 minutes. Full laboratory procedural blanks with combusted sand were performed in parallel with each batch of rocks to ensure that any background signals were negligible in comparison with biomarker analyte abundances found in the rocks (typically by at least 3 orders of magnitude). Saturate hydrocarbon and aromatic fractions for rock bitumens and oils were obtained by silica gel column chromatography; the saturate fractions were eluted with hexane and the aromatic fractions with DCM:hexane (1:1 v/v).

The procedures for ancient biomarker analyses from sedimentary rocks from Huqf Supergroup of the SOSB performed at MIT (results reported in Supplementary Tables 1-2) were similar to those described above for UCR protocols, including MRM-GC-MS methods (see below) which were described in detail previously[S1,S6]. Analytical errors for absolute yields of individual hopanes and steranes are estimated at ± 30%. Average uncertainties in hopane and sterane biomarker ratios are ± 8% as calculated from multiple analyses of a saturated hydrocarbon fraction from AGSO and GeoMark standard oils (n = 30). Full procedural blanks with combusted sand were ran in parallel with each batch of samples to quantify any low background signal. Supplementary Tables 1-2 contain original data from Love *et al.*, 2009[S1]; but now also with 26-mes sterane data added. The yields and ratios verify that significant abundances of 26-mes were detected in all these samples at a similar order of magnitude abundance to those of 24-ipc steranes.

4.2 Sterane analysis using Multiple Reaction Monitoring (MRM)-GC-MS at UCR

Saturated hydrocarbon fractions from ancient rocks and oils as wells as from modern sponge HyPy pyrolysates were analyzed by Multiple Reaction Monitoring-Gas Chromatography-Mass Spectrometry (MRM-GC-MS) conducted at UCR on a Waters Autospec Premier mass spectrometer equipped with an Agilent 7890A gas chromatograph and DB-1MS coated capillary column (60 m x 0.25 mm, 0.25 μm film) using He for carrier gas. Typically, one microliter of an aliphatic sample dissolved in hexane was injected onto the GC column in splitless injection mode. The GC temperature program consisted of an initial hold at 60°C for 2 min, heating to 150°C at 10 °C min^{-1} followed by heating to 320°C at 3°C min^{-1} and a final hold for 22 min. Analyses were performed via splitless injection in electron impact mode, with an ionization energy of 70 eV and an accelerating voltage of 8 kV. MRM transitions for C_{27}–C_{35} hopanes, C_{31}–C_{36} methylhopanes, C_{21}–C_{22} and C_{26}–C_{30} steranes, C_{30} methylsteranes and C_{19}–C_{26} tricyclic terpanes were monitored in the method used. Procedural blanks with pre-combusted sand yielded less than 0.1 ng of individual hopane and sterane isomers per g of combusted sand[S10]. Polycyclic biomarker alkanes (tricyclic terpanes, hopanes, steranes, etc.) were quantified by addition of a deuterated C_{29} sterane standard [d_4-ααα–24-ethylcholestane (20R)] to saturated hydrocarbon fractions and comparison of relative peak areas. In MRM analyses, this standard compound was detected using 404→221 Da ion transition. Cross-talk of non-sterane signal in 414→217 Da ion chromatograms from C_{30} and C_{31} hopanes was < 0.2% of 412→191 Da hopane signal [mainly 17α,21β(H)-hopane, which is resolvable from C_{30} steranes] and <1% of the 426→191 Da signal, respectively[S9].

Peak identifications of sponge steranes were confirmed by comparison of retention times with an AGSO oil saturated hydrocarbon standard and with Neoproterozoic oils from Eastern Siberia[S11,S12] and India[S13] which were reported previously to contain significant quantities of 24-ipc and which we have now demonstrated contain significant quantities of 26-mes (Supplementary Table 3). Polycyclic biomarkers were quantified assuming equal mass spectral response factors between analytes and the d_4-C_{29}-ααα-24-ethylcholestane (20R) internal standard. Analytical errors for absolute yields of individual hopanes and

steranes are estimated at ± 30%. Average uncertainties in hopane and sterane biomarker ratios are ± 8% as calculated from multiple analyses of a saturated hydrocarbon fraction prepared from AGSO and GeoMark Research standard oils (n = 30 MRM analyses).

4.3 Sterane analysis by GC-triple quadrupole (QQQ)-MS at GeoMark Research

To confirm the presence of the new 26-methylstigmastane peak and investigate the retention time of the analyte peaks compared with other C_{30} steranes (24-npc and 24-ipc), the saturated hydrocarbon fractions from sponge HyPy products and oils from Eastern Siberia and India (Supplementary Table 3) were run on a different instrument employing a different GC column to that used in the MRM-GCMS instrument at UCR. GC-QQQ-MS was performed at GeoMark Research (Houston, TX) on an Agilent 7000A Triple Quad interfaced with an Agilent 7890A gas chromatograph equipped with a J&W Scientific capillary column (DB-5MS+DG: 60 m x 0.25 mm i.d., 0.25 μm film thickness, 10 m guard column). Using helium as carrier gas, the flow was programmed from 1.2 mL min^{-1} to 3.2 mL min^{-1}. The GC oven was programmed from 40°C (2 min) to 325°C (25.75 min) at 4°C min^{-1}. Saturated hydrocarbon fractions were spiked with a mixture of 7 internal standards (Chiron Routine Biomarker Internal Standard Cocktail 1). Samples were concentrated without being taken to dryness & were injected in cold splitless mode at 45°C with the injector temperature ramped at 700°C min^{-1} to 300°C. The MS source was operated in EI-mode at 300°C with ionization energy at -70 eV. A number of molecular ion to fragment transitions were monitored throughout the run; dwell time was adjusted as needed to produce 3.5 cycles/second. Exact chromatographic co-elution (with identical retention time in the C_{30} sterane analytical window) of the αααR diastereoisomer of 26-mes sterane in our ancient oils with the equivalent peak from the modern sponges was demonstrated in 414→217 Da ion transitions (the parent molecular mass to daughter fragment ion transition for regular (4-desmethyl) C_{30} sterane compounds).

4.4 Extraction and direct analysis of sterols in modern sponge cells

Eighteen modern sponge samples were acquired for solvent extraction to monitor their free sterol contents (as TMS ethers). Sponge specimens were supplied by co-authors PC

and EAS and their colleagues; including Jean Vacelet, Ute Hentschel, Kevin Peterson, Ted Molinski, Thierry Pérez, Hans Tore Rapp, Alexander Plotkin, Jae-Sang Hong, Yusheng M. Huang, Sven Rohde, Scott Nichols, Barbara Calcinai, Jose V. Lopez, Gulia Gatti, Bartek Ciperling, João-Pedro Fonseca, Luís Magro, Francesca Azzini, Allen G. Collins and the Bedford Institute of Oceanography (Dartmouth, Canada). Sponge biomass arrived immersed in ethanol or freeze-dried. Combined ethanol washings for each sample were filtered to remove suspended particulates, concentrated into a small volume and then transferred to a pre-weighed glass vial and blown down carefully under dry N_2 gas. Freeze-dried sponge biomass was extracted via sonication for 25 minutes in DCM:methanol (3:1 v/v) to recover the total lipid extract.

Total lipid extracts (TLEs) were separated into 3 fractions, based on polarity, by silica gel absorption chromatography. Approximately, 1-5 mg of TLE was adsorbed on the top of a 10 cm silica gel pipette column and then sequentially eluted with 1.5 column volumes of *n*-hexane (fraction 1), 2 column volumes of DCM (fraction 2) and 3 column volumes of DCM:methanol (7:3 v/v) (fraction 3). The alcohol products, including sterols, typically eluted in fraction 2 and approximately 20-50 μg of this fraction was derivatized with 10 μl of bis(trimethylsilyl)trifluoroacetamide (BSTFA) in 10 μl of pyridine at 70ºC for 30 minutes.

Alcohol fractions were then analyzed by GC-MS as trimethylsilyl (TMS) ethers within 36 hours of derivatization in full scan mode at UC-Riverside using gas chromatography-mass spectrometry (GC-MS) on an Agilent 7890A GC system coupled to an Agilent 5975C inert MSD mass spectrometer. Sample solutions were volatilized via programmed-temperature vaporization (PTV) injection onto a DB1-MS capillary column (60 m × 0.32 mm, 0.25 μm film thickness) and helium was used as the carrier gas. The oven temperature program used for GC for the derivatized alcohol fraction consisted of an initial temperature hold at 60°C for 2 min, followed by an increase to 150°C at 20°C min^{-1}, and then a subsequent increase to 325°C at 2°C min^{-1} and held for 20 min. Data was analyzed using ChemStation G10701CA (Version C) software, Agilent Technologies. C_{30} sterol

identifications for the three 26-mes precursors (stelliferasterol (**B13**), isostelliferasterol (**B14**) and strongylosterol (**B15**); Fig. 2) in certain *Rhabdastrella* and *Geodia* sponge species were identified from published mass spectral features and relative retention times[S14-S16]. Stelliferasterol was the dominant C_{30} sterol in *Rhabdastrella globostellata* (PC922, Supplementary Figs. 1-2), while strongylosterol, stelliferasterol and isostelliferasterol were found in *Geodia parva* (GpII).

RESULTS & DISCUSSION

5. Structural identification of 26-mes and self-consistency checks for syngenicity

The structural identification of the 26-mes sterane series was carefully verified by observing perfect co-elution of the peak signal for the ααα*R* diastereoisomer standard produced by HyPy of extant sponges (that contained 26-mes sterols as their major C_{30} sterol constituents) with the ααα*R* diastereoisomer resolvable within the equilibrium mixture in the Neoproterozoic rocks and oils samples (the least altered 5α,14α,17α(H)-20R or ααα*R* sterane form; which is present as the major sterane peak in extant eukaryotes and is one of four abundant regular sterane stereoisomers in ancient geological samples (Fig. 1)). To recover the steranes generated from mild reductive conversion of sponge sterols, HyPy was performed on demosponges containing at least one of the three different known 26-mes sterol precursors (stelliferasterol, isostelliferasterol and strongylosterol; Fig. 2). In all cases for the demosponges in which stelliferasterol/isostelliferasterol/strongylosterol were the most abundant C_{30} sterol constituents, the major C_{30} sterane product was 26-mes (in the form of two resolvable peaks: βαα*R* and a more abundant ααα*R* isomer; e.g. Supplementary Figs. 1-2), facilitating a direct correlation with the ancient steranes using the ααα*R* compound peak (Fig. 1). Various co-injection experiments with subsequent analysis with MRM-GC-MS show conclusively that the ααα*R* sterane product generated by HyPy conversion of these modern sponges exactly matches the ααα*R* isomer from the new sterane series found in the Neoproterozoic-Cambrian rocks and oils and that this is 26-methylstigmastane beyond any reasonable doubt (Supplementary Figs. 2-5).

From a large set of modern sponges (Supplementary Table 4) used for investigation in our study, we identified *Rhabdastrella globostellata* (specimen PC922, Supplementary Tables 4-5) as a model system for a 26-mes sterol producing organisms since it contains one dominant C_{30} sterol that can be unambiguously identified as stelliferasterol[S15,S17,S29] as well as lower amounts of isostelliferasterol (although this Great Barrier reef sponge was mistakenly called *Jaspis stellifera* in these classic papers, the identity of the sponge was later confirmed as *Rhabdastrella globostellata* from detailed sponge taxonomy[S44]) . The *Rhabdastrella globostellata* (specimen PC922, along with others from Taiwan) from our collection contains Δ24(28)-dehydroaplysterol (**B11**) as the main sterol constituent, as we confirmed (Supplementary Figs. 1-2), which is the known biosynthetic C_{29} sterol precursor of stelliferasterol, isostelliferasterol and strongylosterol[S16]. **B11** is also found as the major sterol which makes appreciable amounts of two other 26-mes precursor sterols: stelliferasterol and isostelliferasterol[S17]. Strongylosterol was first reported many years ago as the main sterol constituent of the sponge *Strongylophora* (aka *Petrosia*) *durissima*[S14,S16].

Stelliferasterol has undergone complete structural and stereochemical elucidation[S15, S17,S29] and the NMR and mass spectral details were published in these papers. The basic biosynthetic pathway which requires a concerted triple bioalkylation of the cholesterol (**B1**) sidechain has been studied in detail. Stelliferasterol has been confirmed as 26-methylstigmasta-5,25(26)E-dien-3β-ol which contains 26-methylstigmastane as the basic sterane skeleton (Fig. 2). The efficacy of the HyPy systematics for the reductive conversion of sterols to steranes with minimal structural and stereochemical alteration has been previously demonstrated unequivocally from decades of prior work using model sterol compounds and algal cultures from the published literature[S1,S7,S34,S35]. So, the major C_{30} sterane products from HyPy conversion of PC922 sponge biomass is undoubtedly 26-methylstigmastane (see Fig. 1, Supplementary Figs. 1-2). The proof of concept for sterol to sterane conversions via HyPy of sponge biomass is consistent across C_{27}-C_{30} sterol and stanol compound classes. We have observed that aplysterols/dehydroaplysterols yield aplysterane (βααR and αααR forms; structure **A7** in Chart I; Supplementary Table 5), 24-methylenecholesterol yields ergostane (βααR and αααR forms; structure **A2** in Chart I;

Supplementary Fig. 6), 24-ipc sterols yield 24-ipc steranes (βααR and αααR forms; structure **A5** in Chart I; Fig. 1) and thymosiosterol (structure **C12** in Chart I) yields thymosiosterane (αααR only since there is no double bond at C-5 and 5α(H) is the configuration in the sterol precursor; structure **A8** in Chart I; Fig. 1).

The co-elution of the 5α,14α,17α(H)-20R (αααR) diastereoisomer was confirmed by two different GC-MS techniques performed independently in two different laboratories. Using 414→217 Da ion transitions to detect regular (4-desmethyl) C_{30} steranes, MRM-GC-MS was performed at UCR on a 60 m capillary column with a DB-1MS stationary phase while QQQ-MS was performed at GeoMark Research on a 60 m column with a DB-5MS stationary phase (see **Section 4.1**). With both GC columns, the 26-mes series elutes later than both the 24-npc (**A4**) and 24-ipc sterane series. The chromatographic elution order of the different C_{30} sterane compounds (see Fig. 1 & Supplementary Table 6) is consistent with chromatographic first principles: compounds with all three additional carbon atoms positioned in the interior of the sterane side-chain at position C-24 (i.e. 24-npc and 24-ipc) will elute *before* compounds with extra carbons in terminal sites (i.e. 26-mes and thymosiosterane). Since 26-mes contains two extra mid-chain carbons through an ethyl-substituent at C-24 and one terminal methyl group at C-26, this predicts elution times intermediate between 24-ipc (no extra terminal carbon) and thymosiosterane (two terminal methyl groups both attached at C-26), as is observed (Fig. 1, Supplementary Table 6). Three series of C_{30} steranes are present (24-npc, 24-ipc and now 26-mes) in Neoproterozoic rocks and oils whereas thymosiosterane has not been confirmed as yet from the geological record (Fig. 1). Additionally, partially resolved peaks for the αββR and αββS diastereoisomer forms of ancient 26-mes steranes correctly eluted with the retention times predicted for C_{30} steranes; near but immediately before the immature βααR diastereoisomer from the sponge HyPy products, also consistent with their identities as 26-mes diastereoisomers (Supplementary Fig. 4).

Other than the 24-ipc steranes, no other diagnostic animal molecular biomarkers have been applied to the geological record, till now, that are resolvable from the conventional

steroids found as abundant membrane lipids of extant microbial eukaryotes. This is surprising but largely reflects only an emerging knowledge concerning the variety, abundance and taxonomic distributions of unconventional steroids made predominantly or exclusively by animals that can be preserved as detectable and resolvable ancient sterane markers. Other recalcitrant lipids could expand the molecular biomarker repertoire significantly in the search for early animal fossil evidence. Reactive functional groups, particularly alkene and alcohol groups, associated with sterols do not survive the protracted processes of sedimentary diagenesis and catagenesis and so any diagnostic structural features must be preserved over hundreds of millions of years of burial as an integral part of the recalcitrant hydrocarbon core structure. Animal steroids containing unusually alkylated side-chains offer a high potential in this regard, since a subset of demosponges are known to make a diverse array of these unconventional steroids as secondary metabolites[S18]. 26-mes steroids are such an example of "unconventional" steroids which possess distinctive methylation at the terminus of the steroid sidechain (**A10**) and other structural varieties of these steroids represent promising targets for novel animal markers being detected in the ancient geological record. As more demosponge genomes and transcriptomes are sequenced, future studies may reveal an evolutionary phylogeny for key enzymes involved in biosynthesis of steroids with unusual extended side-chains (i.e. **A8** and **A9**).

The parallel analysis of kerogen-bound products, containing abundant covalently bound 24-ipc and 26-mes (Supplementary Table 2), alongside conventional solvent-extractable biomarkers (Supplementary Table 1) adds significant confidence that these sponge biomarkers are indigenous and syngenetic with the host sediment and have not simply migrated from other, possibly younger, strata. The bound biomarker pool exhibits a slightly less mature distribution of hopanes and steranes than the corresponding solvent extracts for any particular rock, including noticeably less amounts of rearranged hopanes and sterane isomers, such as neohopanes and diasteranes[S7,S19]. This distinguishes the HyPy products from any residual rock bitumen components which may have escaped solvent extraction or any migrated petroleum and confirms that the HyPy-generated biomarkers were predominantly covalently-linked into kerogen. Furthermore, the kerogen-bound biomarker

distributions confirm that kerogen was largely formed early during stages of diagenesis. It is an important self-consistency check that confirms that the three series of C_{30} sterane compounds detected (24-npc, 24-ipc and 26-mes) are genuine Neoproterozoic-Cambrian biomarker compounds and we can rule out any significant contaminant contributions.

6. 26-mes steranes as specific biomarkers for demosponges

Unlike the case for 24-isopropylcholesterol (and related 24-ipc sterols with different unsaturation patterns) which have been found in trace amounts in some (but not all) published sterol assays from pelagophyte algae[S1,S4], no plausible precursor sterols for 26-methylstigmastane have been reported in any extant taxa *other than* from a subset of demosponges. This is despite decades of research in lipid natural products and detailed sterol assays of all major groups of algae[S7,S20-S25] and unicellular animal outgroups[S5,S26]. In contrast to demosponges, previous investigations into the sterol constituents of 20 hexactinellid sponges and 20 calcarean sponges did not reveal the presence of any unconventional steroid structures with unusual side-chain chemistry[S27,S28] and the authors concluded that the main sterols in hexactinellids were derived predominantly from dietary uptake. Nor did we find any detectable 26-mes steranes, even in trace amounts, in this study from MRM-GC-MS analysis of the HyPy products of a hexactinellid sponge, two homoscleromorphs and a calcisponge (Supplementary Table 5).

There has been no report of appropriate 26-mes precursor sterols from any eukaryote lineage, other than from demosponges, despite the finding of these three C_{30} sterol compounds going back 40 years. These sterols (stelliferasterol, isostelliferasterol and strongylosterol) were discovered and their structures and stereochemistries were characterized in detail[S14,S15,S29]. Mass spectra and other spectroscopic attributes were clearly described and published in these papers. If 26-mes precursor sterols were significant sterol constituents of other eukaryotic lineages, then it is puzzling why no reports have followed these papers through this 40-year time lapse given that the information needed to identify these was published and available in established chemistry journals.

More steroid assays are needed on heterotrophic protists, animal outgroups (e.g. refs S5, S26) and other classes of sponges (e.g. refs S27, S28) but an important feature of all these sterol distributions is already recognized. Namely, that no other sponge class (other than the demosponges) or unicellular animal outgroup contains unconventional steroid structures possessing unusual side-chain chemistry (such as terminal methyl groups) of any variety. Only an array of conventional sterols with common straight chain alkylated sidechains (hydrogen, methyl, ethyl, or propyl substituents at C-24) have thus far been found in hexactinellid sponges, calcarean sponges and unicellular animal outgroups.

Our results show that certain species of demosponges from genera *Rhabdastrella* and *Geodia* (family Geodiidae, order Tetractinellida), from shallow tropical to deep arctic waters, make significant amounts of the appropriate precursor sterols with methylation at C-26 in the sterol side-chain amongst their major C_{30} sterols[S14-S16,S29] and correspondingly generated 26-mes as their major C_{30} steranes from HyPy treatment (Supplementary Table 5; Supplementary Figs. 1-2). The three precursor sterols (Fig. 2) for 26-methylstigmatane are stelliferasterol (**B13**), isostelliferasterol (**B14**) and strongylosterol (**B15**). Additionally, we found low but detectable amounts of 26-mes in HyPy products (Supplementary Table 5) from species within genera *Aplysina* and *Verongula* (family Aplysinidae, order Verongiida) as well as one species from genus *Cymbaxinella* (order Agelasida). This suggests that there are likely more demosponge species, within these orders or from different taxonomic groups, that can produce terminally alkylated sterols.

A diverse array of unconventional steroids found in demosponges may reflect necessary membrane structural modifications that accompanied the divergence of this class of poriferans[S11,S30-S32]. The precise role that these unusual sterols, with structural modifications to the side-chain or steroid nucleus, serve in demosponge cell membranes is not known but it has been suggested that they may (i) fulfill a purely structural role by providing improved conformational alignment of cell membrane molecules, including other unusual sponge lipids and proteins, or alternatively, (ii) be involved in modulating a variety of physiological regulatory processes[S33]. Similarly, the synthesis of steroids in sponges is

not fully understood despite decades of research into sponge natural products and the sterols may be derived from one of (or a combination of) three end-member sources: i) synthesized by the host sponge *de novo,* ii) by-products of unique symbiotic relationships between the sponge and specific microbes that it hosts and iii) obtained from dietary uptake and/or are alteration products from a primary stock of sterols. Our view is that the uniformity of unsaturation patterns (double bond positions) across the major sterol constituents in the sponge extracts suggests a host control on the overall assemblage of downstream sterols, though some upstream sterol precursors may be routed from the diet rather than exclusively made *de novo* by the host. This is particularly pertinent to side-chain chemistry and demosponges are now thought to contain "promiscuous" SMT genes that allow them to modify the sterol side-chain[S5].

7. HyPy of extant biomass allows screening of the sterane core content of steroids

Continuous-flow HyPy (described in **Section 3**) was used to reductively convert sterols (and any other functionalized steroids) from sponge cells into steranes (and some sterenes) to facilitate comparison of extant and fossil lipids in the same analytical window. HyPy generation of extant biomass is a useful and rapid means of assessing the diversity and relative abundance of lipid hydrocarbon skeletons[S1,S7]. The key features of the HyPy methodology ensure that covalent bonds can be cleaved at the lowest possible temperatures in the heating cycle (typically between 250^{o}C and 450^{o}C) and a high hydrogen sweep gas flowrate continuously flushes products from the hot zone of the reactor bed, minimizing rearranged by-product compounds. This combination of factors results in excellent preservation of structural and stereochemical features of hydrocarbon products in comparison to other analytical pyrolysis techniques. Cholesterol (**B1**), cholestenol (**C1**) and other lipid model compounds were previously investigated under the standardized HyPy conditions to monitor the level of side-chain cleavage and stereochemical rearrangement during pyrolysis[S34]. The amount of side-chain scission which occurred was found to be very low while excellent retention of the biologically inherited stereochemistry was observed in the sterane products (e.g. 5α,14α,17α(H)-20R isomer of cholestane (**A1**) was the dominant product from 5α,14α,17α(H)-20R cholestenol; while both 5β,14α,17α(H)-20R and

5α,14α,17α(H)-20R isomers are generated from sterols possessing Δ5 unsaturation). Additionally, cholestane products yielded individual $\delta^{13}C$ signatures that matched those of the precursor sterols within analytical error[S35].

As an example, comparing the intact sterol and HyPy sterane profiles of *Geodia hentscheli* shows the efficacy of sterol → sterane conversion from HyPy treatment, retaining the core stereochemical and structural integrity of the hydrocarbon core skeleton with little side-chain cracking and with 5β,14α,17α(H)-20R and 5α,14α,17α(H)-20R isomers generated (Supplementary Fig. 6). *Geodia hentscheli* produced ergostane (**A2**) as its major sterane from HyPy conversion (Supplementary Table 5). GC-MS analysis of the derivatized sterols (as TMS ethers using BSTFA) in the total lipid extracts independently confirmed that the same specimen contained 24-methylenecholesterol (a conventional C_{28} sterol) as its major sterol component and that the total relative abundance of each steroid class ($C_{27}/C_{28}/C_{29}$) agrees between the two analytical approaches (Supplementary Fig. 6). This illustrates the effective conversion of the biological precursor sterol to the saturated sterane 'core skeleton' after HyPy treatment and provides the basis for comparisons between modern and ancient sponge-derived biomarkers since both contain the ααα*R* diastereoisomer peak (e.g. Fig. 1).

The major patterns of HyPy-generated sterane distributions from a variety of modern sponge species (Supplementary Table 4) are represented by the data displayed in Supplementary Table 5. The HyPy approach allows a very sensitive screening for any individual sterane compounds using MRM-GC-MS of HyPy products, down to sub-ng quantities. This allows us to assess the sterane core content of steroids in biomass by a rapid and reproducible process[S7], particularly in this case to identify sponges that contain significant quantities of 26-mes steroids (Supplementary Table 5) and allows for a direct comparison with ancient steranes in the geological record (Fig. 1). Sponges in our collection that contained either stelliferasterol (**B13**), isostelliferasterol (**B14**) and/or strongylosterol (**B15**) (e.g. *Geodia parva*, *Rhabdastrella globostellata*, *Geodia phlegraei*) as major Δ5-unsaturated C_{30} sterols gave 26-methylstigmastane (**A10**) as the major HyPy

C_{30} sterane product (0.5 to 9.3% of total C_{27}-C_{30} steranes) in every case, without exception (Supplementary Table 5). As expected, the 26-mes sterane peaks from these three sponges resulted in two major stereoisomer peaks from the reduction of the double bond at C-5 in each precursor sterol: 5β,14α,17α(H)-20R (βααR) and 5α,14α,17α(H)-20R (αααR). These are the two main sterane diastereoisomers produced from the reduction of any conventional or unconventional sterols with unsaturation at C-5 position (Supplementary Fig. 3). The same pattern is seen from HyPy of sponges that yield conventional sterols and steranes (e.g. *Geodia hentscheli*, Supplementary Fig. 6). Furthermore, HyPy screening of microalgal cultures has yet to produce any C_{30} sterane series consistent with a 26-mes source, and conventional steroids dominate the HyPy products with sterane carbon number patterns generally matching the sterol patterns reported in the literature[S7].

8. The enigma of strongylosterol and host sponge association in some previous reports

Strongylosterol was first isolated from a sponge specimen collected on Laing island, 35 meters water depth (Papua New Guinea) and identified by Dr. P. A. Thomas as *Petrosia (Strongylophora) durissima*[S14]. However, when we investigated another specimen of *P. (S.) durissima* from Indonesia (PC1068), we could not detect 26-mes in the HyPy products [as expected if it produced strongylosterol in high amounts, as suggested by ref. S14]. Furthermore, we obtained the same result from the holotype of *Petrosia (Strongylophora) durissima* (NHM 1907.2.1.37) from Sri Lanka. We can therefore assume that strongylosterol was isolated from a different species, mis-identified as *P. (S.) durissima* by Dr. Thomas. Unfortunately, no voucher has been kept from the previous study[S14], so we cannot be sure of that. Therefore, we consider that Bortolotto *et al.* (1978)[S14] worked on a species that we call *P. (S.)* cf. *durissima* in the present study.

The chemist J. C. Braekman had given pieces of the whole Papua New Guinea sponge collection to Dr. Thomas to identify. Dr. Thomas described this sponge collection in a subsequent series of papers. Thomas (1991)[S36] describes from this collection *Strongylophora durissima* along with a new species, *Strongylophora septata*. Both species have identical spicules but different external shapes. Thomas (1991)[S36] unfortunately does

not mention which one had been studied by Bortolotto *et al.* (1978)[S14] but according to our results, we can assume that strongylosterol was originally isolated from *P. (S.) septeta* and not *P. (S.) durissima*. Again, we cannot formally conclude due to the absence of vouchers left from Bortolotto *et al.* (1978)[S14].

9. *Jaspis wondoensis* versus *Rhabdastrella wondoensis*

Jaspis is a contentious group of sponges currently belonging to the Ancorinidae family, Tetractinellida order[S37]. *Jaspis wondoensis*[S38] was described from the shallow waters of Geomun islands (locality of Wondo), Jeju Strait, South Korea. In this study we examined material from the Jeju Strait, Yeoseo Island (courtesy of Dr. Jae-Sang Hong, Inha University, Republic of Korea). *Jaspis* species are characterized by oxeas of different sizes (notably microxeas on the surface) with a paratangential arrangement; euasters are without a centrum. However, we observed spicules (rare large spherasters in the cortex, no microxeas) and spicule arrangement (radial organization) suggesting that this species should be reallocated to the genus *Rhabdastrella,* as *Rhabdastrella wondoensis* comb. nov. The absence of triaenes in *R. wondoensis*, is not uncommon in some *Rhabdastrella* species (e.g. *R. globostellata*). Molecular phylogeny studies further suggest that the tropical *Rhabdastrella* genus belongs to the Geodiidae family, and not to the Ancorinidae family[S37].

10. Plausible sponge sterane biomarkers predating the Sturtian glaciation (>717 Ma)

26-methylcholestane (a C_{28} sterane, structure **A6**), informally designated as cryostane[S39,S40] is an unusual sterane biomarker which has been detected in certain pre-Sturtian (pre-717 Ma) Neoproterozoic rocks that contain C_{27} steranes as their major steranes[S39-S42]. Here we note that 24-ipc and 26-mes (C_{30} steranes) are found in rocks/oils that often exhibit a C_{29} sterane dominance[S1,S6,S12,this study]. This carbon number relationship (n+1 versus n) may be from heterotrophic modification (n+1) of primary steroids (n) in these ancient marine environments systems and suggests dietary modification of sterol feedstocks as a possible early transformation mechanism to make unconventional steroids. Based on this C_{28} sterane (cryostane) being the terminal methylation product of cholestane (C_{27} regular sterane), it is plausible that crysotane is a biomarker for the earliest sponges or

their ancestors and is analogous to 26-mes being from stigmastane (C_{29} regular sterane; **A3**). The arguments are currently substantially weaker for cryostane versus 24-ipc and 26-mes, however, since precursor sterols containing a cryostane core structure have not yet been reported from any modern taxa. Therefore, we cannot say if the precursor lipids are exclusive to demosponges. It is possible though that cryostane may be a marker for ancient sponges or for a unicellular stem metazoan[S39] or derived from heterotrophic unicellular protists[S43]. The origins of cryostane are intriguing and a bridging of the cryostane and 26-mes/24-ipc records may signify a continuity of sponge markers persisting through the two Neoproterozoic glaciation events (Fig. 3), but this requires further investigation.

SUPPLEMENTARY FIGURE CAPTIONS

Supplementary Figure 1. Total ion current (TIC) chromatograms showing the distribution of sterols in the alcohol fractions from total lipid extracts of four different specimens of *Rhabdastrella globostellata* from Taiwan. Sterols were derivatized and analyzed as trimethylsilyl (TMS) ethers. Peak assignments 1: C_{27} Δ5 cholesterol; 2: C_{28} Δ5,25 codisterol; 3: C_{29} Δ5,24(28)-dehydroaplysterol; 4: C_{30} Δ5,25 stelliferasterol.

Supplementary Figure 2. A. Selected ion chromatogram (m/z 129) from GCMS of a sponge sterol extract shows the sterol distributions (as TMS ethers) of *Rhabdastrella globostellata* PC922 and **B.** the associated mass spectrum of the main C_{30} sterol, stelliferasterol (*). Major fragment ions and fragment ion abundances for strongylosterol from our sponge *R. globostellata* PC922 are in close agreement with previously published spectra of stelliferasterol[S15,S17.S29], and prior full spectroscopic characterization confirm its structure and stereochemistry as 26-methylstigmasta-5,25(26)-dien-3β-ol) which yields **C.** 26-methylstigmastane (βαα20R and ααα20R) as the dominant C_{30} sterane from HyPy.

Supplementary Figure 3. Mass spectra of the two major sterane isomers (5β,14α,17α(H),20R; βααR and 5α,14α,17α(H),20R; αααR) of stigmastane and 26-mes generated from HyPy of modern sponges (Supplementary Table 5). Mass spectra **A** and **C** show characteristic fragment patterns of αααR isomers of 26-mes and stigmastane from GCMS using electron ionization (70 eV), respectively. Mass spectra **B** and **D** show characteristic fragment patterns of βααR 26-mes and stigmastane, respectively, and exhibit elevated 151 Da relative to 149 Da fragment response for the βααR stereoisomer for both compounds as expected. Designation of α (below the plane) and β (above the plane) hydrogen configurations are shown using open and closed circles, respectively.

Supplementary Figure 4. MRM-GCMS (414→217 Da) chromatograms of (*top*) two Ediacaran-Cambrian oils with different C_{30} sterane distributions that show a mature/geologic distribution of regular sterane isomers (αααS, αββR, αββS, αααR) and

(*middle*) a sponge from our dataset that produces 26-mes as its major C_{30} sterane with an immature distribution of sterane isomers (only βααR and αααR) (see Supplementary Tables 3-4 for sample info). The (*bottom*) co-injection of the immature sterane series from the sponge with the mature sterane series from the two oils confirms the presence of 26-mes in rock bitumens and oils ranging from Cryogenian to Early Cambrian in age (black shaded 26-mes αααR peak becomes greatly enhanced). Consistent with first principle elution patterns, this co-injection experiment shows that the immature 26-mes βααR peak elutes slightly *after* the mature 26-mes αββ(R+S) doublet as a right shoulder peak; a feature similar to our observations for other sterane compounds (e.g. stigmastane and 24-ipc). C_{30} sterane series assignments: 24-npc (o/gray shaded peak); 24-ipc (+/gray shaded peak); 26-mes (*/black shaded peak).

Supplementary Figure 5. MRM-GCMS (414→217 Da) chromatograms of the C_{30} regular sterane distributions for two Ediacaran-Cambrian oils used in this study employing two different heating methods (see Supplementary Table 3 for sample details). The regular method (*top*) with a temperature ramp of 3°C min^{-1} to 320°C results in only weakly resolved αββ(R+S) peaks for *both* 24-npc and 26-mes. A revised GC method (*bottom*) with a slower temperature ramp of 2°C min^{-1} to 320°C greatly enhances the separation of the αββ(R+S) doublet for *both* 24-npc and 26-mes. C_{30} sterane series assignments: 24-npc (o); 24-ipc (+); 26-mes (*). Blue shaded peaks; αββ(R+S) stereoisomers. Red shaded peaks; ααα(S+R) stereoisomers.

Supplementary Figure 6. Extracted sterols (as TMS ethers) vs HyPy-generated sterane distributions for the same demosponge specimen of *Geodia hentscheli*. The similar abundances patterns between the intact sterols and their sterane products highlights the efficacy of HyPy conversion of precursor steroids in extant sponge biomass to immature steranes with minimal thermal cracking and rearrangements (forming predominantly βααR and αααR diastereoisomers from Δ5-sterols).

SUPPLEMENTARY REFERENCES

S1. Love, G. D. *et al.* Fossil steroids record the appearance of Demospongiae during the Cryogenian period. *Nature* **457**, 718-721 (2009).

S2. Brocks, J. J. & Butterfield, N. J. Biogeochemistry: Early animals out in the cold. *Nature* **457**, 672-673 (2009).

S3. Antcliffe, J. B. Questioning the Evidence of Organic Compounds Called Sponge Biomarkers. *Palaeontology* **56**, 917-925 (2013).

S4. Love, G. D. & Summons, R. E. The molecular record of Cryogenian sponges - a response to Antcliffe (2013). *Palaeontology* **58**, 1131-1136 (2015).

S5. Gold, D. A. *et al.* Sterol and genomic analyses validate the sponge biomarker hypothesis. *P Natl Acad Sci USA* **113**, 2684-2689 (2016).

S6. Grosjean, E., Love, G. D., Stalvies, C., Fike, D. A. & Summons, R. E. Origin of petroleum in the Neoproterozoic-Cambrian South Oman Salt Basin. *Org Geochem* **40**, 87-110 (2009).

S7. Love, G. D. *et al.* A catalytic hydropyrolysis method for the rapid screening of microbial cultures for lipid biomarkers. *Org Geochem* **36**, 63-82 (2005).

S8. Rohrssen, M., Love, G. D., Fischer, W., Finnegan, S. & Fike, D. A. Lipid biomarkers record fundamental changes in the microbial community structure of tropical seas during the Late Ordovician Hirnantian glaciation. *Geology* **41**, 127-130 (2013).

S9. Rohrssen, M., Gill, B. C. & Love, G. D. Scarcity of the C-30 sterane biomarker, 24-n-propylcholestane, in Lower Paleozoic marine paleoenvironments. *Org Geochem* **80**, 1-7 (2015).

S10. Haddad, E. E. *et al.* Lipid biomarker stratigraphic records through the Late Devonian Frasnian/Famennian boundary: Comparison of high-and low-latitude epicontinental marine settings. *Org Geochem* **98**, 38-53 (2016).

S11. Mccaffrey, M. A. *et al.* Paleoenvironmental Implications of Novel C-30 Steranes in Precambrian to Cenozoic Age Petroleum and Bitumen. *Geochim Cosmochim Ac* **58**, 529-532 (1994).

S12. Kelly, A. E., Love, G. D., Zumberge, J. E. & Summons, R. E. Hydrocarbon biomarkers of Neoproterozoic to Lower Cambrian oils from eastern Siberia. *Org Geochem* **42**, 640-654 (2011).

S13. Peters, K. E., Clark, M. E., Dasgupta, U., Mccaffrey, M. A. & Lee, C. Y. Recognition of an Infracambrian Source-Rock Based on Biomarkers in the Bahewala-1 Oil, India. *Aapg Bulletin-American Association of Petroleum Geologists* **79**, 1481-1494 (1995).

S14. Bortolotto, M., Braekman, J. C., Daloze, D. & Tursch, B. Chemical Studies of Marine-Invertebrates. 36. Strongylosterol, a Novel C-30 Sterol from Sponge Strongylophora-Durissima Dendy. *B Soc Chim Belg* **87**, 539-543 (1978).

S15. Theobald, N., Wells, R. J. & Djerassi, C. Minor and Trace Sterols in Marine-Invertebrates .8. Isolation, Structure Elucidation, and Partial Synthesis of 2 Novel Sterols - Stelliferasterol and Isostelliferasterol. *J Am Chem Soc* **100**, 7677-7684 (1978).

S16. Stoilov, I. L., Thompson, J. E., Cho, J. H. & Djerassi, C. Biosynthetic-Studies of Marine Lipids .9. Stereochemical Aspects and Hydrogen Migrations in the

Biosynthesis of the Triply Alkylated Side-Chain of the Sponge Sterol Strongylosterol. *J Am Chem Soc* **108**, 8235-8241 (1986).
S17. Cho, J. H., Thompson, J. E., Stoilov, I. L., Djerassi, C. Biosynthetic studies of marine lipids. 14. 24(28)-Dehydroaplysterol and other sponge sterols from Jaspis stellifera. *J Org Chem* **53**, 3466-3469 (1988).
S18. Kerr, R. G. & Baker, B. J. Marine Sterols. *Nat Prod Rep* **8**, 465-497 (1991).
S19. Murray, I. P., Love, G. D., Snape, C. E. & Bailey, N. J. L. Comparison of covalently-bound aliphatic biomarkers released via hydropyrolysis with their solvent-extractable counterparts for a suite of Kimmeridge clays. *Org Geochem* **29**, 1487-1505 (1998).
S20. Volkman, J. K., Barrett, S. M., Dunstan, G. A. & Jeffrey, S. W. Sterol Biomarkers for Microalgae from the Green Algal Class Prasinophyceae. *Org Geochem* **21**, 1211-1218 (1994).
S21. Kodner, R. B., Pearson, A., Summons, R. E. & Knoll, A. H. Sterols in red and green algae: quantification, phylogeny, and relevance for the interpretation of geologic steranes. *Geobiology* **6**, 411-420 (2008).
S22. Giner, J. L., Zhao, H., Boyer, G. L., Satchwell, M. F. & Andersen, R. A. Sterol Chemotaxonomy of Marine Pelagophyte Algae. *Chem Biodivers* **6**, 1111-1130 (2009).
S23. Volkman, J. K. A Review of Sterol Markers for Marine and Terrigenous Organic-Matter. *Org Geochem* **9**, 83-99 (1986).
S24. Volkman, J. K. Sterols in microorganisms. *Appl Microbiol Biot* **60**, 495-506 (2003).
S25. Volkman, J. K. *et al.* Microalgal biomarkers: A review of recent research developments. *Org Geochem* **29**, 1163-1179 (1998).
S26. Kodner, R. B., Summons, R. E., Pearson, A., King, N. & Knoll, A. H. Sterols in a unicellular relative of the metazoans. *P Natl Acad Sci USA* **105**, 9897-9902 (2008).
S27. Blumenberg, M., Thiel, V., Pape, T. & Michaelis, W. The steroids of hexactinellid sponges. *Naturwissenschaften* **89**, 415-419 (2002).
S28. Hagemann, A., Voigt, O., Wörheide, G., Thiel, V. The sterols of calcareous sponges (Calcarea, Porifera). *Chem & Phys Lipids* **156**, 26-2 (2008).
S29. Theobald, N. & Djerassi, C. Determination of Absolute-Configuration of Stelliferasterol and Strongylosterol - 2 Marine Sterols with Extended Side-Chains. *Tetrahedron Lett*, 4369-4372 (1978).
S30. Itoh, T., Sica, D. & Djerassi, C. Minor and Trace Sterols in Marine-Invertebrates .35. Isolation and Structure Elucidation of 74 Sterols from the Sponge Axinella-Cannabina. *J Chem Soc Perk T 1*, 147-153 (1983).
S31. Rambabu, M. & Sarma, N. S. Chemistry of Herbacin and New Unusual Sterols from Marine Sponge Dysidea-Herbacea. *Indian J Chem B* **26**, 1156-1160 (1987).
S32. Hofheinz, W. & Oesterhelt, G. 24-Isopropylcholesterol and "22-Dehydro-24-Isopropylcholesterol, Novel Sterols from a Sponge. *Helv Chim Acta* **62**, 1307-1309 (1979).
S33. Lawson, M. P., Thompson, J. E. & Djerassi, C. Phospholipid Studies of Marine Organisms .19. Localization of Long-Chain Fatty-Acids and Unconventional Sterols in Spherulous Cells of a Marine Sponge. *Lipids* **23**, 1037-1048 (1988).

S34. Meredith, W., Sun, C. G., Snape, C. E., Sephton, M. A. & Love, G. D. The use of model compounds to investigate the release of covalently bound biomarkers via hydropyrolysis. *Org Geochem* **37**, 1705-1714 (2006).
S35. Sephton, M. A., Meredith, W., Sun, C. G. & Snape, C. E. Hydropyrolysis of steroids: a preparative step for compound-specific carbon isotope ratio analysis. *Rapid Commun Mass Sp* **19**, 3339-3342 (2005).
S36. Thomas, P.A. Sponges of Papua and New Guinea-Part order Haplosclerida Topsent. *J Mar Biol Ass India* **33**, 308-316 (1991).
S37. Cárdenas, P., Xavier, J. R., Reveillaud, J., Schander, C. & Rapp, H. T. Molecular Phylogeny of the Astrophorida (Porifera, *Demospongiae*(rho)) Reveals an Unexpected High Level of Spicule Homoplasy. *Plos One* **6**, (2011).
S38. Sim, C.J. & Kim, Y.-A. A systematic study on the marine sponges in Korea: 12. Tetractinomorpha (Porifera: Demospongiae). *Korean J Sys Zoo* **11**, 147-158 (1995).
S39. Brocks, J. J. *et al.* Early sponges and toxic protists: possible sources of cryostane, an age diagnostic biomarker antedating Sturtian Snowball Earth. *Geobiology* **14**, 129-149 (2016).
S40. Adam, P., Schaeffer, P., Brocks, J. J. Synthesis of 26-methyl cholestane and identification of cryostane in mid-Neoproterozoic sediments. *Org Geochem* **115**, 246-249 (2018).
S41. Summons, R. E. *et al.* Distinctive Hydrocarbon Biomarkers from Fossiliferous Sediment of the Late Proterozoic Walcott Member, Chuar Group, Grand-Canyon, Arizona. *Geochim Cosmochim Ac* **52**, 2625-2637 (1988).
S42. Vogel, M.B., Moldowan, J.M. & Zinniker, D. Biomarkers from Units in the Uinta Mountain and Chuar Groups. *Utah Geo Assc Pub* **33**, 75-96 (2005).
S43. Brocks, J. J. *et al.* The rise of algae in Cryogenian oceans and the emergence of animals. *Nature* **548**, 578-581 (2017).
S44. Kennedy, J.A. Resolving the '*Jaspis stellifera*' complex. *Mem. Queensl. Mus*. **45**, 453-476 (2000).

Supplementary Figure 1

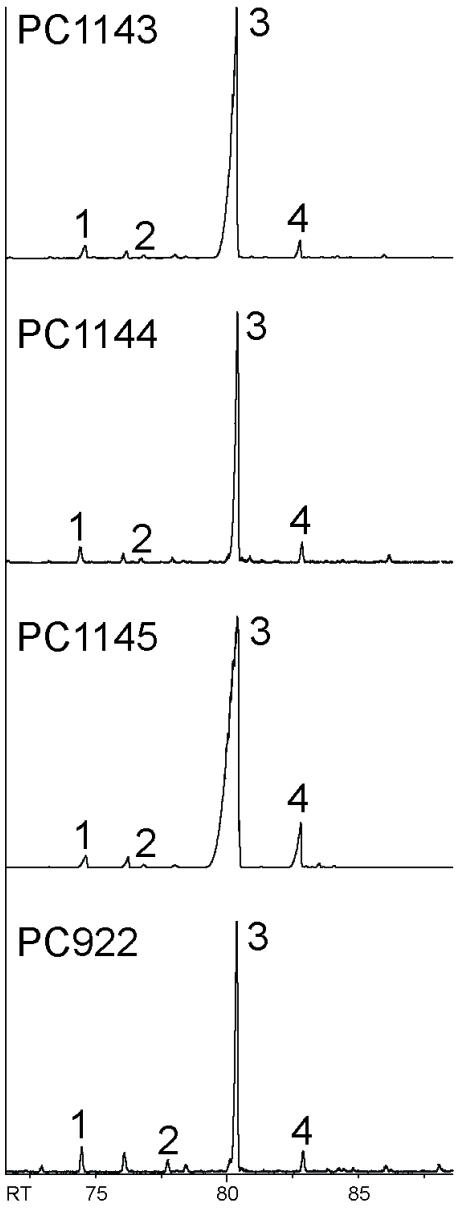

Supplementary Figure 2

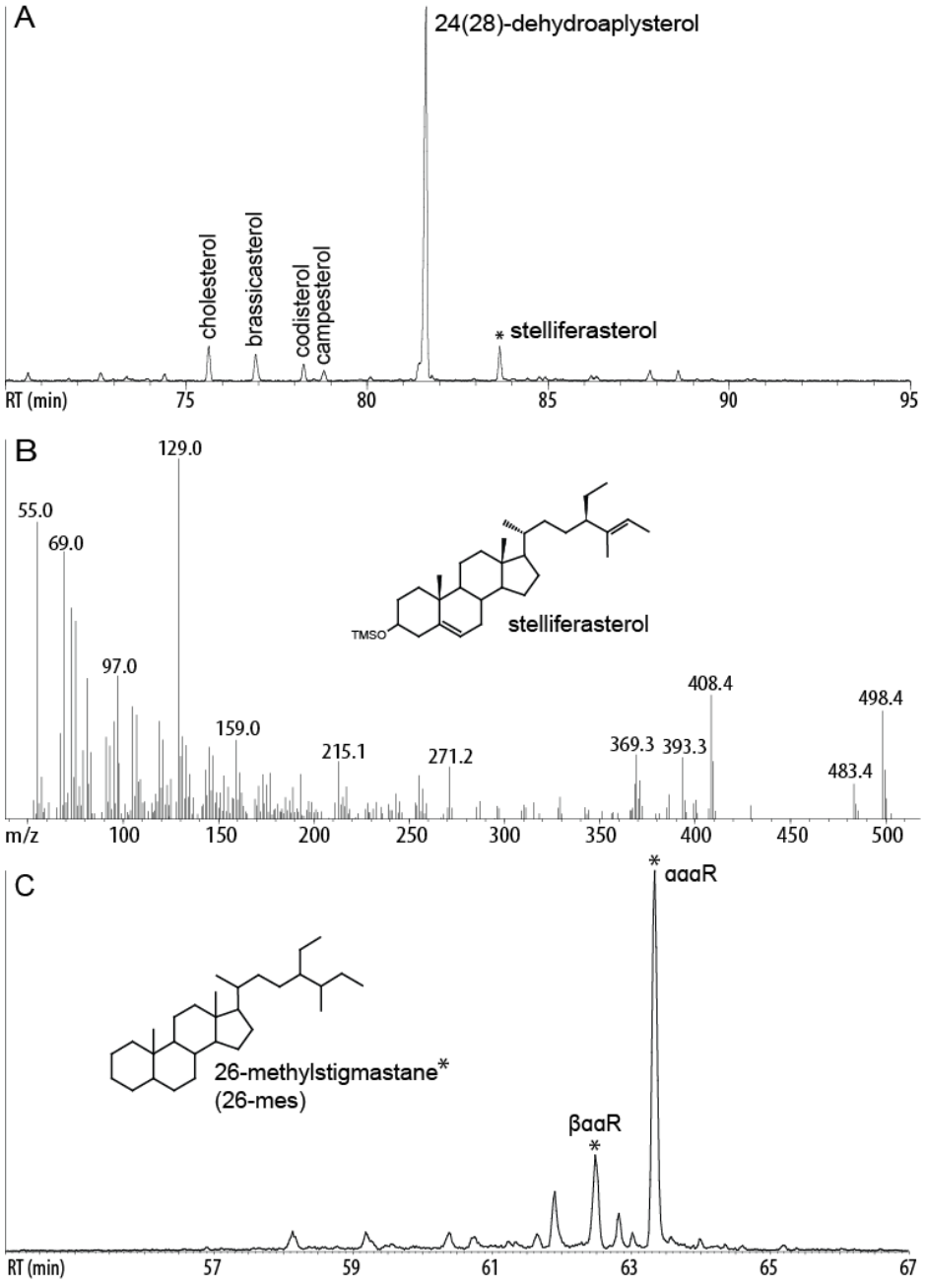

Supplementary Figure 3

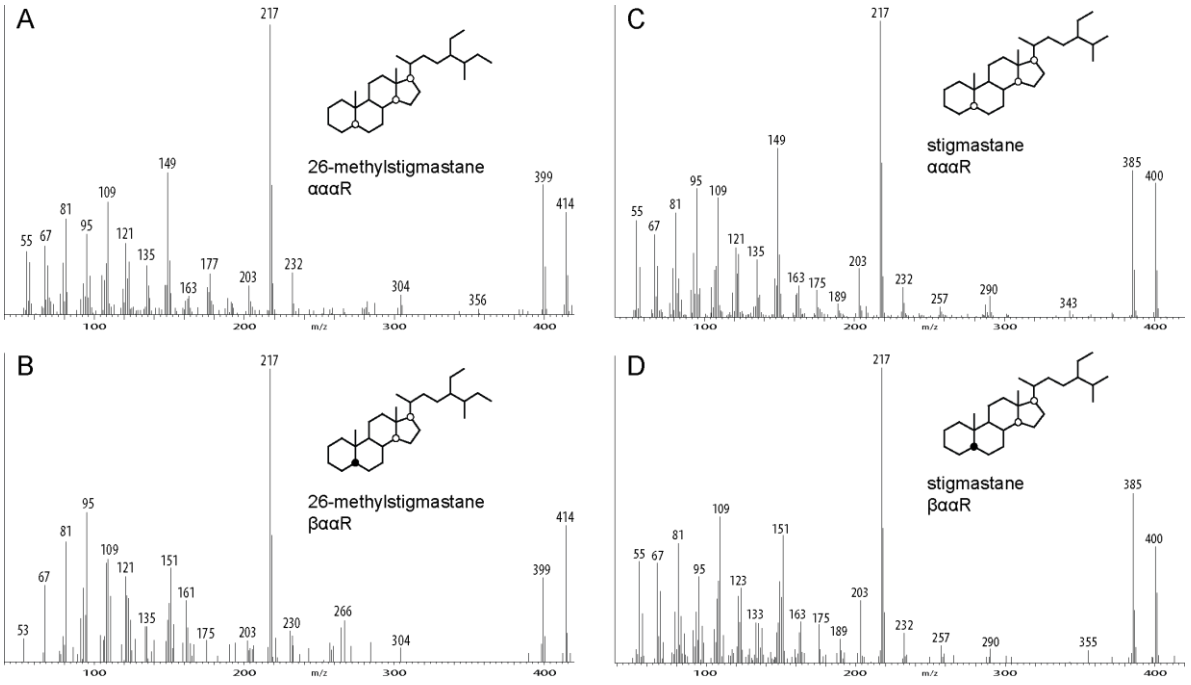

Supplementary Figure 4

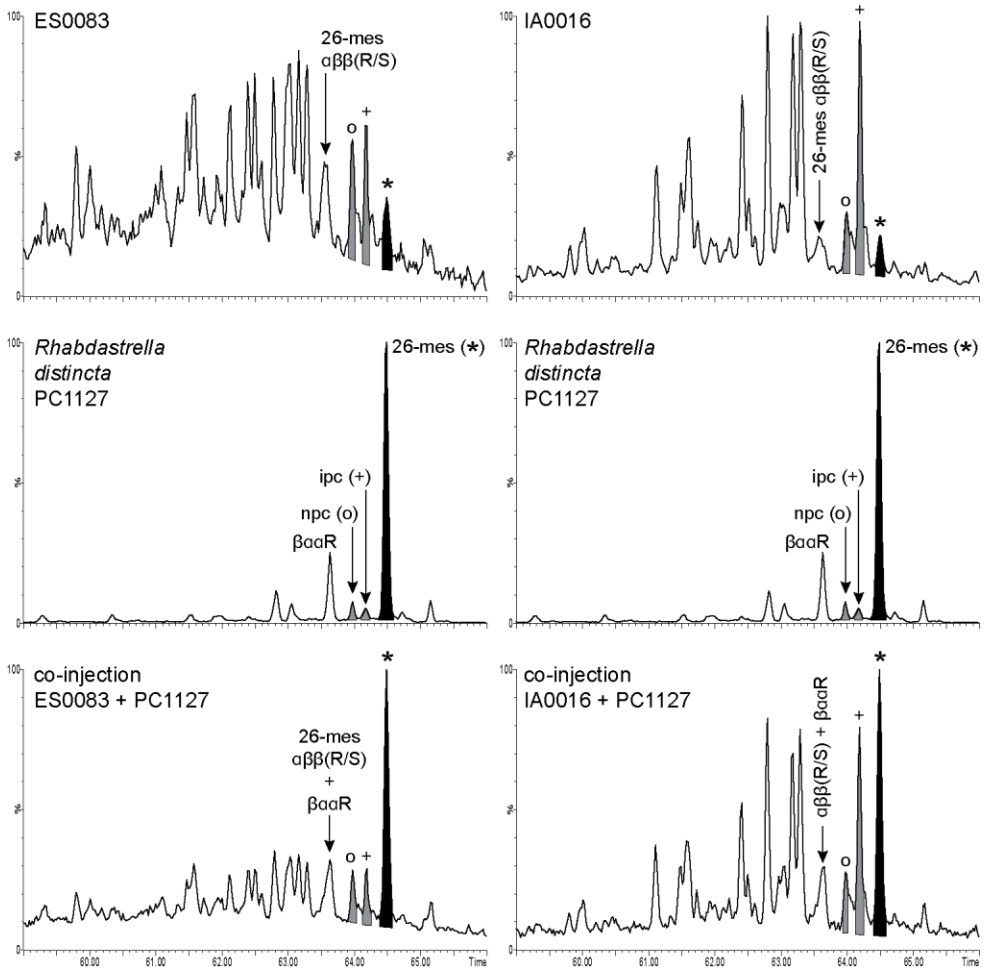

Supplementary Figure 5

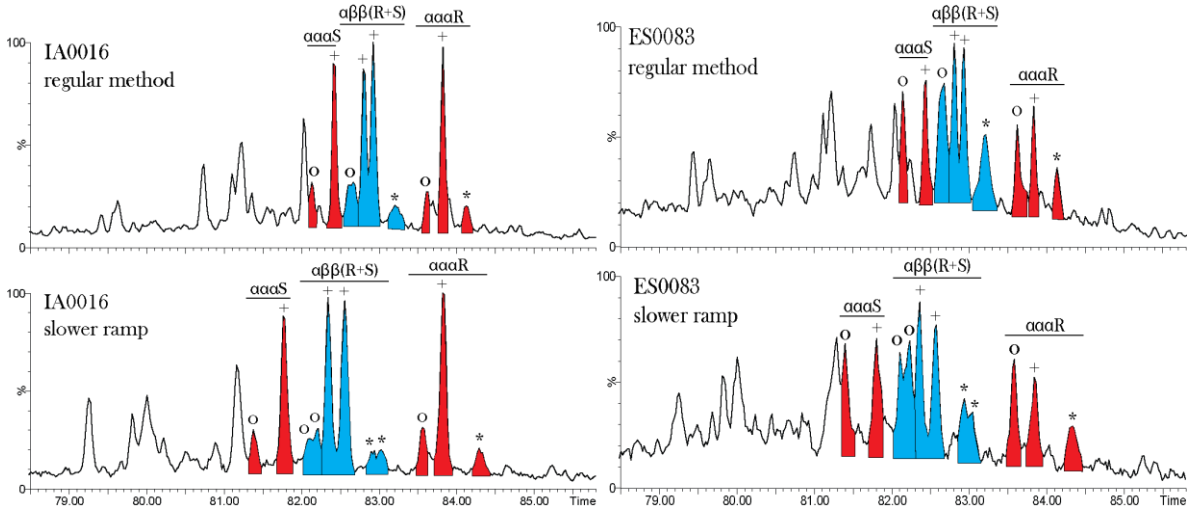

Supplementary Figure 6

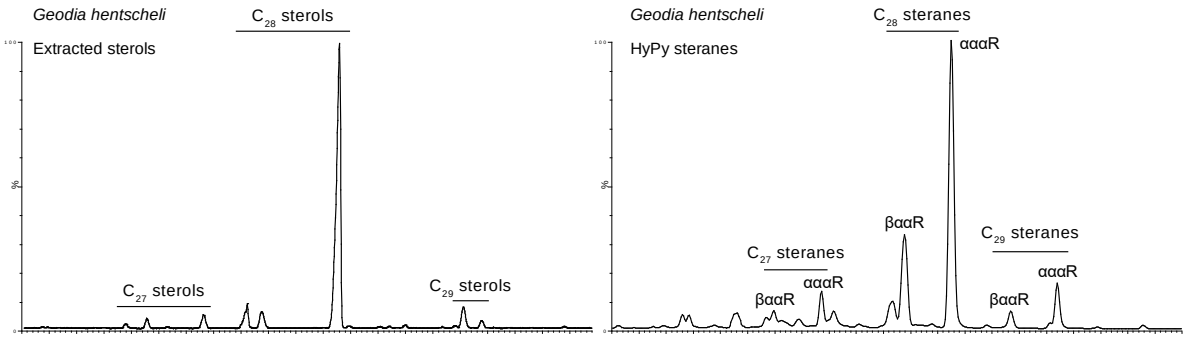

Chart I

Conventional

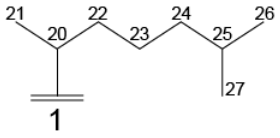

1

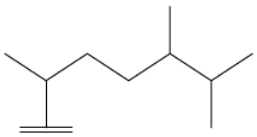

2

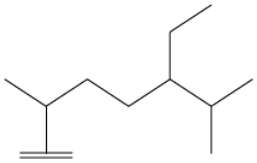

3

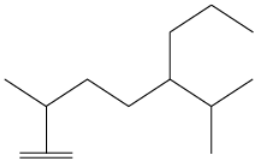

4

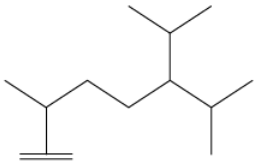

5

Unconventional

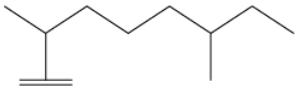

6

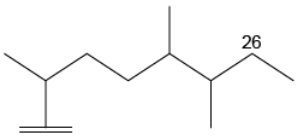

7

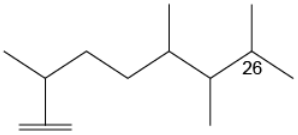

8

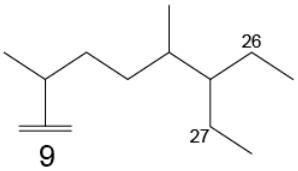

9

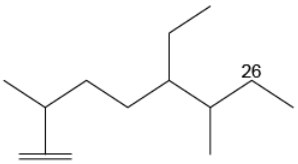

10

Unsaturated

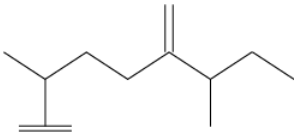

11

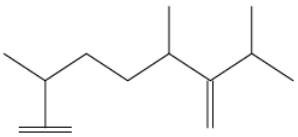

12

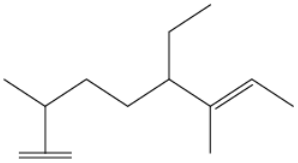

13

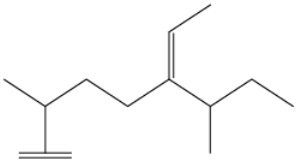

14

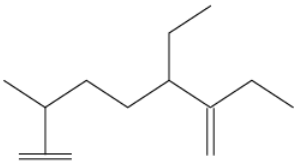

15

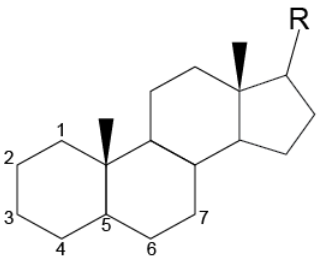

A

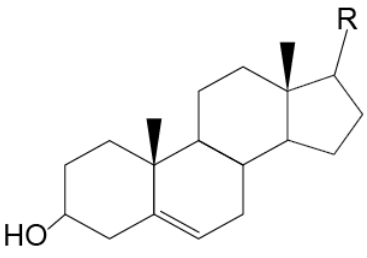

B

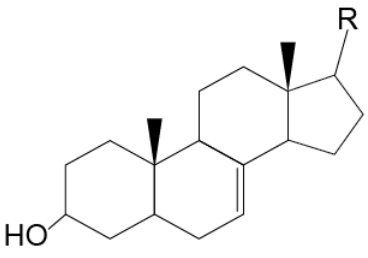

C

Supplementary Table 1: Selected biomarker ratios and yields obtained from free saturate fractions of sediment cores and cuttings

See separate SI Document “Supplementary Table 1”

Supplementary Table 2: Selected biomarker ratios and yields obtained from hydropyrolysis of kerogens/extracted sediments

Well ID	Min. Depth (m)	Strat.	TOC wt%	Lithology/Facies	S/H[a]	%C_{26} st[b]	%C_{29} st[c]	%C_{30} st[d]	ipc/npc[e]	ipc[e] ppm sats	26-mes[f] ppm sats	26-mes/ ipc[f]
OMR-1	2851	A5C	0.44	Carbonate stringer	0.89	5.62	59	2.27	0.83	61.8	30.5	0.49
BB-3	2928	A4C	1.06	Carbonate stringer	0.84	8.27	53	3.60	0.73	14.7	13.8	0.94
DRR-1	2990	A3C	0.44	Carbonate stringer	0.80	7.99	62	1.88	0.82	15.6	12.7	0.82
RF-1	3547	A2C*	n.d.	Carbonate stringer- saline*	0.62	4.68	68	2.87	0.84	8.4	5.0	0.59
SJT-1	5033	A2C	0.86	Carbonate, pustular laminite	0.93	9.80	52	3.16	0.64	5.2	0.3	0.06
SJT-1	5053	A2C	1.39	Carbonate, thrombolite	1.04	10.1	55	3.64	1.10	5.6	2.1	0.37
DHS-3	2997	A1C	1.22	Carbonate stringer	0.77	6.42	69	2.88	0.96	18.6	9.4	0.51
MIN-1	3400	A1C*	n.d.	Carbonate stringer- saline facies*	0.58	3.98	70	2.15	1.35	11.6	4.9	0.42
SB-1	1569-1602	Buah	2.3	Marlstone?	0.89	12.9	63	1.34	0.53	4.4	5.4	1.24
AMSE-1	2345-2375	Buah	1.6	Carbonate	1.12	10.5	67	1.91	0.72	4.2	2.4	0.57
ZFR-1	1905-1940	Shuram	3.4	Mudstone/siltstone	0.99	12.9	60	2.71	0.66	14.1	17.2	1.22
SNK-1	930-990	Shuram	n.d.	Mudstone/siltstone, Lower Shuram	0.55	13.3	58	4.58	1.35	2.7	1.3	0.49
JF-1	2648-2676	Masirah B	n.d.	Mudstone/siltstone, Upper Masirah	0.73	14.2	55	5.60	1.35	3.8	2.6	0.69
HNR-1	2026-2060	Masirah B	n.d.	Mudstone/sitstone, Upper Masirah	1.21	12.0	54	3.43	1.52	2.4	1.7	0.70
GM-1	2420-2446	Ghad. Manquil	0.59	Laminated lime mudstone	0.68	9.70	66	3.04	1.31	6.2	3.5	0.56
Athel Group												
AM-9	1731	Thuleilat	2.2	Black shale	0.97	9.89	57	2.46	1.24	12.0	10.1	0.84
MAR-248	2068-2084	Thuleilat	10.4	Mudstone/silicylite transitional	2.49	15.8	65	2.00	0.74	16.3	16.5	1.01
MAR-248	2104-2120	Silicylite	3.4	Upper silicylite	2.10	12.4	69	2.25	0.69	11.2	11.0	0.99
MAR-248	2240-2352	Silicylite	2.3	Lower silicylite	1.46	6.73	75	2.08	1.05	34.3	26.5	0.77
MAR-248	2420-2460	U shale	6.4	Black shale	1.19	13.2	53	2.71	1.66	9.5	6.4	0.67

a: ratio of (C_{27}-C_{29} steranes)/ (C_{27}+ $C_{29\text{-}35}$ hopanes)
b: ratio of (21-nor- +27-norcholestanes)/Σ(C_{26}-C_{29} steranes), for C_{26} desmethylsteranes (C_{27}-C_{29} 21-norsteranes peak areas were not included)
c: ratio of C_{29} steranes to the total sum of C_{27}-C_{29} steranes
d: ratio of (24-*n*-propylcholestanes +24-isopropylcholestanes)/Σ(C_{27}-C_{30} steranes) for C_{30} desmethylsteranes
e: ratios and compound yields were calculated from summing peak areas of all 4 regular isomers of each compound ($\alpha\alpha\alpha$S, $\alpha\beta\beta$R, $\alpha\beta\beta$S, $\alpha\alpha\alpha$R)
f: ratios and compound yields for 26-methylstigamstane (26-mes) were calculated from the peak area of the $\alpha\alpha\alpha$R isomer
n.d. not determined
*: elevated salinity and marine facies
Analytical errors with 27-norcholestane and 24-isopropylcholestane absolute yields are estimated at ± 30%. Average uncertainties in hopane and sterane biomarker ratios are ± 8% as calculated from multiple analyses of a saturated hydrocarbon fraction prepared from an AGSO standard oil (n = 30 MRM analyses).
Note: All products from HyPy were monitored to ensure that the bulk of the biomarkers generated were released by cleavage of covalent bonds and were not simply residual bitumen components. This was achieved by observing only very low or nil amounts of certain rearranged steranes and hopanes found exclusively as free hydrocarbons. For example, for all HyPy analyses here (Ts/Tm) <0.15, (diasteranes/regular steranes) <0.1 with much reduced levels of 28,30-bisnorhopanes relative to total hopanes compared with the corresponding free extracts.

Supplementary Table 3: C_{30} sterane abundances and distributions in a selection of rocks and oils through geologic time

Age	SampleID	Location	Type	TOC (wt%)	Lithology/Facies	Basin/Fm./Gp./Well	Major Sterane[a]	%C_{30}[b]	ipc/npc[c]	26-mes/ipc[c]	26-mes/npc[c]
Ediacaran	OMO005[#]	Oman	oil	N/A		A1C	stigmastane	2.6%	1.35	0.45	0.61
	OMO003[#]	Oman	oil	N/A		PS Huqf	stigmastane	3.9%	1.44	0.50	0.72
	OMO014[#]	Oman	oil	N/A		PS Huqf	stigmastane	3.7%	0.64	0.68	0.43
	ES0001[$]	E. Siberia	oil	N/A		Kamov Gp.	stigmastane	2.3%	1.03	0.35	0.36
	ES0053[$]	E. Siberia	oil	N/A		Byuk	stigmastane	2.3%	1.73	0.40	0.70
Cambrian	IA0016[*]	India	oil	N/A		Baghewala-1	stigmastane	2.0%	4.42	0.23	1.01
	OMO043[#]	Oman	oil	N/A		A5C	stigmastane	3.1%	1.73	0.36	0.62
	ES0083[$]	E. Siberia	oil	N/A		Usol'ye	stigmastane	2.4%	1.03	0.64	0.66
Ordovician	VA-23[%]	Nevada, USA	rock	18.4	Shale	Vinini	stigmastane	0.2%	n.d.	n.d.	n.d.
	SGH-43.0[%]	Indiana, USA	rock	0.2	Arg. carbonate	Liberty/Whitewater	stigmastane	0.1%	n.d.	n.d.	n.d.
Silurian	901-16.0[%]	Anticosti, Canada	rock	0.2	Carbonate	Becscie	stigmastane	0.1%	n.d.	n.d.	n.d.
	G1+2.0[%]	Gotland, Sweden	rock	0.2	Marlstone	Visby	stigmastane	0.6%	n.d.	n.d.	n.d.
Devonian	Pando1[^]	Bolivia	rock	5.6	Shale	Madre de Dios	stigmastane	1.5%	0.16	0.98	0.16
	Pando4[^]	Bolivia	rock	9.5	Shale	Madre de Dios	stigmastane	3.0%	0.16	1.00	0.17
	Pando12[^]	Bolivia	rock	11.8	Shale	Madre de Dios	stigmastane	2.7%	0.25	0.57	0.14
	Pando18[^]	Bolivia	rock	18.8	Shale	Madre de Dios	stigmastane	4.1%	0.27	0.52	0.14
	OK0620[*]	Oklahoma, USA	oil	N/A		Arnold 2-17H	stigmastane	3.6%	0.16	0.64	0.11
	OK0621[*]	Oklahoma, USA	oil	N/A		Sabre 1-7H	stigmastane	2.7%	0.10	1.15	0.12
Permian	M22[*]	China	rock	n.d.	Micrite	Maokou Fm.	stigmastane	3.4%	0.78	0.68	0.26
	W13[*]	China	rock	n.d.	Micrite	Wujchaping Fm.	stigmastane	2.5%	0.58	0.46	0.23
Jurassic	JR13[*]	United Kingdom	rock	8.9	Shale	Jet Rock	cholestane	4.9%	0.11	0.00	0.00
	8022[*]	North Sea	oil	N/A		Clair	cholestane	7.3%	0.13	0.00	0.00
Cretaceous	207-1258A[+]	Suriname	rock	10.8	Shale	Demerara Rise	cholestane	6.3%	0.12	0.00	0.00
	207-1258B[+]	Suriname	rock	14.7	Shale	Demerara Rise	cholestane	4.4%	0.13	0.00	0.00
	207-1258C[+]	Suriname	rock	1.8	Shale	Demerara Rise	cholestane	7.1%	0.11	0.00	0.00
Phanerozoic Avg. (oil standards)	GeoMark	-	oil	N/A		Mixed oil	stigmastane	1.5%	0.00	n.d.	0.00
	AGSO	-	oil	N/A		Mixed oil	stigmastane	3.3%	0.00	n.d.	0.00
Procedural Blank	Blank sats1	-	-			-	-	0.0%	-	-	-
	Blank sats2	-	-			-	-	0.0%	-	-	-

a: cholestane/ergostane/stigmastane ($C_{27}/C_{28}/C_{29}$) predominance using all the major diastereoisomer forms present

b: Expressed as a % total of C_{27}-C_{30} steranes calculated from summing peak areas of all 4 regular isomers of each C_{30} sterane compound ($\alpha\alpha\alpha$S, $\alpha\beta\beta$R, $\alpha\beta\beta$S, $\alpha\alpha\alpha$R)

c: C_{30} sterane ratio for $\alpha\alpha\alpha$R isomer from MRM-GCMS; ipc, 24-isopropylcholestane; npc, 24-n-propylcholestane; 26-mes, 26-methylcholestane

n.d.: proportions were not detected as overall C_{30} sterane abundances are very low in some early Paleozoic rocks (Rohrssen et al., 2015) with 24-ipc and 26-mes absent

#Grosjean et al., 2009; $Kelly et al., 2011; %Rohrssen et al., 2015; ^Haddad et al., 2016; +Owens et al., 2016; *Love Lab sample (UCR)

Permian rocks M22 & W13 have appreciable amounts of siliceous sponge spicules (unpublished data) with high amount of 24-ipc & 26-mes biomarkers

Supplementary Table 4: Taxonomic assignments for the sponges used in this study

Class	Order	Family	*Genus species*	locality	depth (m)	Collection ID/ Museum accession#
Demospongiae	Tetractinellida	Geodiidae	*Geodia phlegraei*	Svalbard	215	PC511/ ZMBN 89719
			Geodia parva	Flemish Cap, off Newfoundland	1180	PC535/ UPSZMC 78274
			Geodia parva	Mohns Ridge, Greenland Sea	1834-1863	GpII
			Geodia hentscheli	Kolbeinsey Ridge, Greenland Sea	145-215	GhII
			Rhabdastrella distincta	North Sulawesi, Indonesia	27	PC1127
			Rhabdastrella wondoensis	Yeoseo Island, South Korea	shallow	PC866
			Rhabdastrella wondoensis	Yeoseo Island, South Korea	shallow	PC865
			Rhabdastrella globostellata	Penghu Archipelago, Taiwan	shallow	PC922
			Rhabdastrella globostellata	Manus Island, Papua New Guinea	shallow	PC140/ UCMPWC1072
			Rhabdastrella globostellata	Guam Island	shallow	PC492
			Stelletta tuberosa	Flemish Cap, off Newfoundland	1339	PC675
		Tetillidae	*Cinachyrella kuekenthali*	Broward county, Florida	shallow	PC941
			Craniella zetlandica	Korsfjord, Norway	310	PC667
	Haplosclerida	Petrosiidae	*Petrosia (Strongylophora)* cf. *vansoesti*	off Lagos, SW Portugal	60	PC982
			Petrosia (Strongylophora) durissima	North Sulawesi, Indonesia	20	PC1068
			Petrosia (Strongylophora) durissima	Sri Lanka	n/a	NHMUK 1907.2.1.37
	Suberitida	Halichondriidae	*Ciocalypta carballoi*	Rhodes, Greece	15	PC1064
			Halichondria sp.[a]	Marine Biological Laboratory, MA	shallow	sponge 1
		Suberitidae	*Suberites* sp.[a]	Marine Biological Laboratory, MA	shallow	sponge 2
	Bubarida	Bubaridae	*Phakellia ventilabrum*	Tjärnö, Sweden	n/a	FKOG-POR2
	Chondrillida	Chondrillidae	*Thymosiopsis conglomerans*	Tremies cave, Marseille, France	12	Tremies
			Thymosiopsis cf. *cuticulatus*	Endoume cave, Marseille, France	7	Endoume
	Verongiida	Aplysinidae	*Aplysina aerophoba*			TLE430
			Aplysina fulva	Bocas del Toro, Panama	3	A. fulva
			Verongula rigida	Bocas del Toro, Panama	3	sponge 8
			Verongula reiswigi	Bocas del Toro, Panama	3	BT13
	Agelasida	Agelasidae	*Cymbaxinella corrugata*[a]			1153725
	Dictyoceratida	Dysideidae	*Dysidea fragilis*[a]			D. fragilis
	Clionaida	Clionaidae	*Cliona* sp.[a]			sponge 3
	Poecilosclerida	Microcionidae	*Microciona* sp.[a]	Marine Biological Laboratory, MA	shallow	sponge 4
Homoscleromorpha	Homosclerophorida	Plakinidae	*Plakinastrella onkodes*[b]	off Panama, Caribbean Sea	shallow	1133732
			Plakortis halichondrioides[b]	off Panama, Caribbean Sea	shallow	1133720
Hexactinellida	Lyssacinosida	Rossellidae	*Vazella pourtalesii*	Emerald Basin, off Nova Scotia	183-212	HUD16-019-B0362
Calcarea	Leucosolenida	Leucosoleniidae	*Leucosolenia* sp.[a]	Marine Biological Laboratory, MA	shallow	sponge 5

a: from Love et al., 2009
b: curtesy of Allen G. Collins, Smithsonian National Museum of Natural History
UCMPWC: University of California Museum of Paleontology, Berkeley, CA; UPSZMC: Zoological Museum of Uppsala, Sweden
ZMBN: Bergen Museum, Norway; NHMUK: The Natural History Museum, London, UK

Supplementary Table 5: C_{30} regular (4-desmethyl) sterane patterns from catalytic hydropyrolysis (HyPy) of the sponges used in this study

See separate SI Document “Supplementary Table 5”

Supplementary Table 6: GC retention times offsets for various ααα*R* steranes using MRM-GCMS with our standard GC conditions[5]

#C[1]	Sterane[2]	RRT[3]	Alkylation at[4]:
27	cholestane	0.00	-
28	ergostane	2.39	C-24
	cryostane[+]	2.77	C-26
29	stigmastane	4.33	C-24
	aplysterane[#]	4.77	C-24,26
30	24-npc	5.92	C-24
	24-ipc	6.13	C-24
	26-mes	6.43	C-24,26
	verongulasterane[^,#]	6.68	C-24,26,27
	thymosiosterane[^,%]	6.71	C-24,26,26'

1: total number of carbons in each compound
2: for ααα*R* isomer of each sterane; 24-npc = 24-n-propylcholestane;24-ipc = 24-isopropylcholestane; 26-mes =26-methylstigmastane; aplysterane = 24,26-dimethylcholestane
3: RRT = GC Retention time (min) offset relative to cholestane (ααα*R*); standard deviation +/- 0.02 min
4: site of alkylation on the sterane side-chain
5: The GC temperature program consisted of an initial hold at 60°C for 2 min, heating to 150°C at 10 °C/min followed by heating to 320°C at 3°C/min and a final hold for 22 min using a 60 m DB-1MS capillary column (60 m x 0.25 mm, 0.25 µm film) with He as carrier gas
^co-elution of ααα*R* peaks for verongulasterane (24,26,27-trimethylcholestane) and thymosiosterane (24,26,26'-trimethylcholestane)
[+]Brocks et al., 2017; [#]Kokke et al., 1978; [%]Vacelet et al., 2000

Supplementary Table 1: Selected biomarker ratios and yields obtained from free saturate fractions of sediment cores and cuttings

Well ID	Min. Depth (m)	Strat.	TOC wt%	Lithology/Facies	S/H[a]	%C_{26} st[b]	%C_{29} st[c]	%C_{30} st[d]	ipc/npc[e]	ipc[e] ppm sats	26-mes[f] ppm sats	26-mes/ ipc[f]
MKS-2	1648	A6	n.d.	Shale band above A5C stringer	0.82	6.46	58	2.05	1.15	138.7	126.5	0.91
SAR-2	3838	A6*	n.d.	Silicilclastics above A5C stringer	0.21*	6.88*	69	6.69*	1.95	65.6	37.9	0.58
AJB-1	3588	A5C*	n.d.	Carbonate stringer-saline*	0.22*	9.96*	62	1.89*	0.95	13.0	4.7	0.36
OMR-1	2851	A5C	0.44	Carbonate stringer	0.85	6.62	69	1.93	1.55	23.5	10.8	0.46
OMR-1	2853	A5C	1.05	Carbonate stringer	0.82	4.81	69	2.02	1.67	17.7	6.5	0.37
BB-3	2928	A4C	1.06	Carbonate, sapropelic laminite	0.91	4.86	70	2.11	1.49	7.2	5.0	0.69
BB-3	2930	A4C	0.95	Carbonate stringer	1.05	6.26	68	2.45	1.36	11.6	7.8	0.67
BB-5	3009	A4C	1.92	Carbonate stringer	0.99	4.36	66	1.95	1.39	9.2	6.0	0.65
BB-2	2927	A3C	0.53	Carbonate stringer	0.96	4.73	75	2.10	1.49	13.5	8.4	0.62
BBN-1	3785	A3C	0.13	Carbonate stringer	0.79	5.92	70	2.02	1.38	49.0	16.7	0.34
BBN-1	3787	A3C	0.72	Carbonate stringer	0.87	12.7	69	2.31	1.46	11.8	7.1	0.61
BBN-1	3789	A3C	0.40	Carbonate stringer	0.78	5.36	71	2.10	1.66	23.9	10.0	0.42
BBN-1	3790	A3C	0.19	Carbonate stringer	0.82	3.92	70	2.10	1.67	25.5	12.5	0.49
DRR-1	2969	A3C	0.19	Carbonate, crinkly laminite	0.82	4.77	70	2.00	1.45	55.0	26.2	0.48
DRR-1	2990	A3C	0.46	Carbonate, crinkly laminite	0.78	4.56	70	2.07	1.60	62.5	32.4	0.52
BBN-1	4204	A2C	1.90	Carbonate stringer	0.96	6.03	75	2.13	1.52	9.5	5.3	0.55
RF-1	3547	A2C*	n.d.	Carbonate stringer- saline*	0.57	12.9*	70	3.56*	1.17	39.9	16.1	0.40
RF-1	3577	A2C*	n.d.	Carbonate stringer- saline*	0.59	10.1*	72	4.65*	1.48	57.7	28.8	0.50
SAB 1	2399	A2C	1.19	Carbonate stringer	0.93	4.46	75	1.90	1.69	11.9	5.3	0.45
SJT-1	5033	A2C	0.86	Carbonate, pustular laminite	0.72	4.94	52	2.84	1.26	27.4	7.8	0.29
SJT-1	5053	A2C	1.39	Carbonate, thrombolite	0.83	4.74	61	3.39	1.77	33.9	11.5	0.34
DHS-3	2997	A1C	1.22	Carbonate stringer	0.72	4.52	73	1.80	1.92	78.6	30.9	0.39
MIN-1	3400	A1C*	n.d.	Carbonate stringer-saline*	0.52*	9.88*	73	4.75*	1.42	59.4	24.8	0.42
MIN-1	3430	A1C*	n.d.	Carbonate stringer- saline *	0.54*	9.62*	71	5.20*	1.49	116.7	48.7	0.42
AMSE-1	2345-2375	Buah	1.6	Carbonate	0.76	4.07	73	1.66	0.86	5.8	5.4	0.93
SB-1	1569-1602	Buah	2.3	Marlstone?	0.74	8.04	72	1.33	0.77	10.9	11.0	1.01
TRF-2	4411	Buah	3.1	Marlstone	0.84	7.39	67	1.74	0.70	8.7	10.2	1.17
ATH-1	2016-2019	Buah	11.0	Organic-rich marlstone	1.06	9.16	64	1.82	0.55	21.3	27.6	1.29
ZFR-1	1905-1940	Shuram	3.4	Mudstone/siltstone	0.61	6.27	71	2.33	1.78	92.6	43.5	0.47
ATH-1	2379	Shuram	1.5	Mudstone/siltstone	0.56	3.02	77	2.01	0.81	109.1	49.6	0.45
ATH-1	2053-2121	Shuram	1.3	Mudstone/siltstone	0.96	3.81	68	2.12	0.92	14.0	10.1	0.72
ATH-1	2424.5-2447	Shuram	3.0	Mudstone/siltstone	0.66	2.86	70	2.19	1.10	6.8	6.2	0.91
ATH-1	2449-2452	Shuram	3.6	Mudstone/siltstone	0.70	6.68	65	2.50	1.41	8.0	4.5	0.57
TF-1	2247.5-2250	Shuram	n.d.	Mudstone/siltstone	1.06	6.17	65	1.87	1.07	34.3	31.2	0.91
TM-6	2350	Shuram	2.4	Mudstone/siltstone	1.00	5.63	70	2.18	0.92	35.6	28.8	0.81
TM-6	2685-2740	Shuram	3.9	Mudstone/siltstone	0.80	6.15	70	2.00	1.33	26.1	19.6	0.75
TM-6	2800	Shuram	9.2	Lower Shuram black shale	0.84	5.17	73	2.02	1.27	43.5	15.4	0.35
TM-6	2830	Khufai	3.2	Carbonate	0.49	6.02	72	3.34	1.43	72.3	41.3	0.57
RNB-1	3125-3143	Masirah B	1.7	Mudstone/siltstone	0.49	6.84	58	3.53	3.98	14.5	6.8	0.47
ZFR-1	2280-2295	Masirah B	3.8	Mudstone/siltstone	0.73	5.18	84	12.61	16.1	245.7	24.9	0.10
SRS -1	4230-4385	Masirah B	0.4	Mudstone/siltstone	0.70	5.70	64	2.25	1.49	6.1	3.1	0.51

TM-6	2895-2910	Masirah B	4.9	Mudstone/siltstone	0.70	4.49	69	3.16	1.35	12.1	6.9	0.57
MWB-1	2628-2724	Masirah B	n.d.	Mudstone/siltstone	0.73	4.86	60	2.44	1.52	16.5	8.2	0.50
GM-1	2420-2446	Ghad. Manquil	0.59	Laminated lime mudstone	0.90	7.18	72	2.65	3.26	61.0	25.3	0.41
MQR-1	4370	Ghad. Manquil	n.d.	Siltstone	0.43	4.32#	56#	3.72#	0.52#	n.d.	n.d.	0.16
Athel Group												
AML-9	1731	Thuleilat	2.2	Black shale	0.95	11.4	60	2.78	1.34	79.3	41.6	0.52
ATH-1	1000-1102	Thuleilat	8.0	Black shale	0.62	5.74	67	3.34	1.36	18.3	16.1	0.88
MAR-248	2068-2084	Thuleilat	10.4	Mudstone/silicylite transitional	1.29	5.41	71	1.91	1.37	34.8	25.0	0.72
TLT-2	1417.5-1483	Thuleilat	6.4	Black shale	0.81	4.86	71	2.23	1.35	24.9	24.9	1.00
TLT-2	1520-1547	Thuleilat	2.5	Mudstone	0.91	5.16	73	2.27	1.56	35.4	31.5	0.89
ATH-1	1198-1425	Silicylite	3.4	Finely laminated quartz	0.79	4.06	74	1.85	1.39	62.6	37.6	0.60
MAR-248	2104-2120	Silicylite	3.4	Upper silicylite- laminated quartz	1.50	4.78	72	1.93	1.42	28.6	18.3	0.64
MAR-248	2240-2352	Silicylite	2.3	Lower silicylite- laminated quartz	1.02	4.93	76	1.84	1.87	61.0	25.5	0.42
TLT-2	1551-1602	Silicylite	4.3	Finely laminated quartz	1.21	6.11	74	2.41	2.13	90.0	35.6	0.40
TLT-2	1628-1742	Silicylite	2.6	Finely laminated quartz	0.87	21.4	75	2.25	2.44	103.5	38.9	0.38
ATH-1	1425-1527	U shale	3.5	Black shale	0.85	7.73	66	2.37	1.11	17.2	12.2	0.71
ATH-1	1527	U shale	4.9	Black shale	1.00	4.69	61	2.64	0.93	10.0	8.9	0.89
ATH-1	1773-1872	U shale	5.7	Black shale	0.91	19.7	61	2.63	0.78	4.3	3.3	0.77
MAR-248	2420-2460	U shale	6.4	Black shale	0.79	7.24	60	2.90	1.35	8.7	5.4	0.62
TLT-2	1751-1833	U shale	4.0	Black shale	0.89	9.87	65	2.20	1.41	27.9	15.7	0.56

a: ratio of (C_{27}-C_{29} steranes)/ (C_{27}+ $C_{29\text{-}35}$ hopanes)
b: ratio of (21-nor- +27-norcholestanes)/Σ(C_{26}-C_{29} steranes), for C_{26} desmethylsteranes (C_{27}-C_{29} 21-norsteranes peak areas were not included)
c: ratio of C_{29} steranes to the total sum of C_{27}-C_{29} steranes
d: ratio of (24-*n*-propylcholestanes +24-isopropylcholestanes)/Σ(C_{27}-C_{30} steranes), for C_{30} desmethylsteranes
e: ratios and compound yields were calculated from summing peak areas of all 4 regular isomers of each compound ($\alpha\alpha\alpha$S, $\alpha\beta\beta$R, $\alpha\beta\beta$S, $\alpha\alpha\alpha$R)
f: ratios and compound yields for 26-methylstigamstane were calculated from the peak area of the $\alpha\alpha\alpha$R isomer
#: affected by contamination from marine Phanerozoic-sourced petroleum drilling fluids, hence the lower ratios of %C_{29} sterane and iso-C_{30}/n-C_{30} sterane
*: saline marine facies, hence lower sterane/hopane ratio and apparently higher %C_{26} and %C_{30} steranes (as C_{28} and C_{29} 21-norsteranes, prominent at higher salinity, are not included in the calculation)
n.d. not determined
Analytical errors for absolute yields of 27-norcholestanes and 24-isopropylcholestanes absolute yields are estimated at ± 30%. Average uncertainties in hopane and sterane biomarker ratios are ± 8% as calculated from multiple analyses of a saturated hydrocarbon fraction prepared from an AGSO standard oil (n = 30 MRM analyses).
Rock-Eval pyrolysis data for these samples is given in Grosjean et al., (2009).

Supplementary Table 5: C_{30} regular (4-desmethyl) sterane patterns from catalytic hydropyrolysis (HyPy) of the sponges used in this study

Genus species	Major HyPy sterane	Major HyPy C_{30} sterane	24-npc	24-ipc	26-mes	%26-mes[a]	%C_{30} steranes[a]	%Conventional[e]	%Unconventional[b]	TAR[c]
Geodia phlegraei	aplysterane	26-mes	✓	✓	✓	4.0%	5.1%	25.6%	74.4%	2.9
Geodia parva (PC535)	aplysterane	26-mes	✓	✓	✓	4.5%	6.8%	30.9%	69.1%	2.2
Geodia parva (GpII)	aplysterane	26-mes	✓	✓	✓	3.6%	5.4%	32.7%	67.3%	2.1
Geodia hentscheli	ergostane	24-npc	✓	x	x	0.0%	0.9%	100.0%	0.0%	0.0
Rhabdastrella distincta	aplysterane	26-mes	✓	✓	✓	3.8%	4.4%	22.5%	77.5%	3.5
Rhabdastrella wondoensis (PC866)	aplysterane	26-mes	✓	✓	✓	4.1%	5.2%	43.7%	56.3%	1.3
Rhabdastrella wondoensis (PC865)	aplysterane	26-mes	✓	✓	✓	4.4%	5.0%	51.0%	49.0%	1.0
Rhabdastrella globostellata (PC922)	aplysterane	26-mes	✓	✓	✓	9.3%	10.6%	47.8%	52.2%	1.1
Rhabdastrella globostellata (PC140)	stigmastane	26-mes	✓	✓	✓	2.9%	3.9%	69.5%	30.5%	0.5
Rhabdastrella globostellata (PC492)	stigmastane	26-mes	✓	✓	✓	0.5%	0.6%	95.7%	4.3%	0.1
Stelletta tuberosa	ergostane	24-npc	✓	✓	x	0.0%	0.6%	99.6%	0.4%	<0.01
Cinachyrella kuekenthali	stigmastane	24-npc	✓	✓	x	0.0%	0.3%	99.6%	0.4%	<0.01
Craniella zetlandica	stigmastane	24-npc	✓	✓	x	0.0%	0.6%	100.0%	0.0%	0.0
Petrosia (Strongylophora) cf. *vansoesti*	stigmastane	24-npc	✓	x	x	0.0%	1.2%	72.8%	27.2%	0.4
Petrosia (Strongylophora) durissima (PC1068)	stigmastane	24-ipc	✓	✓	x	0.0%	0.7%	100.0%	0.0%	0.0
Petrosia (Strongylophora) durissima (1907.2.1.37)	stigmastane	24-npc	✓	✓	x	0.0%	0.5%	100.0%	0.0%	0.0
Ciocalypta carballoi	24-ipc	24-ipc	✓	✓	x	0.0%	41.6%	99.8%	0.2%	<0.01
Halichondria sp.[d]	cholestane	24-npc	✓	x	x	0.0%	0.2%	100.0%	0.0%	0.0
Suberites sp.[d]	cholestane	24-npc	✓	x	x	0.0%	0.4%	100.0%	0.0%	0.0
Phakellia ventilabrum	cholestane	24-npc	✓	x	x	0.0%	0.8%	100.0%	0.0%	0.0
Thymosiopsis conglomerans	thymosiosterane	thymosiosterane	x	x	x	0.0%	53.5%	43.4%	56.6%	1.3
Thymosiopsis cf. *cuticulatus*	cholestane	24-ipc	✓	✓	x	0.0%	0.7%	99.9%	0.1%	<0.01
Aplysina aerophoba	aplysterane	verongulasterane	✓	✓	✓	0.06%	1.8%	27.9%	72.1%	2.6
Aplysina fulva	aplysterane	verongulasterane	✓	✓	✓	0.03%	1.3%	35.8%	64.2%	1.8
Verongula rigida	cholestane	verongulasterane	✓	✓	✓	0.15%	4.4%	66.6%	33.4%	0.5
Verongula reiswigi	aplysterane	verongulasterane	✓	✓	✓	0.10%	2.9%	62.6%	37.4%	0.6
Cymbaxinella corrugata[d]	cholestane	24-npc	✓	✓	✓	0.12%	1.6%	97.1%	2.9%	0.1
Dysidea fragilis[d]	cholestane	24-npc	✓	✓	x	0.0%	0.4%	98.9%	1.1%	<0.01
Cliona sp.[d]	cholestane	24-npc	✓	x	x	0.0%	0.3%	100.0%	0.0%	0.0
Microciona sp.[d]	cholestane	none	x	x	x	0.0%	0.0%	100.0%	0.0%	0.0
Plakinastrella onkodes	cholestane	none	x	x	x	0.0%	0.0%	100.0%	0.0%	0.0
Plakortis halichondrioides	stigmastane	none	x	x	x	0.0%	0.0%	100.0%	0.0%	0.0
Vazella pourtalesii	cholestane	24-npc	✓	x	x	0.0%	0.2%	100.0%	0.0%	0.0
Leucosolenia sp.[d]	cholestane	none	x	x	x	0.0%	0.0%	100.0%	0.0%	0.0

a: Expressed as a % total of C_{27}-C_{30} steranes for ααR isomer from MRM-GCMS
b: Unconventional = alkylation at [terminal] position C-26 or C-27 in the sterane side-chain (e.g. 26-mes, aplysterane, verongulasterane, thymosiosterane, cryostane)
c: TAR = Terminal Alkylation Ratio = Σ(terminally alkylated steranes)/ Σ(C-24 alkylated steranes)
e: Conventional = cholestane, ergostane, stigmastane, 24-npc and 24-ipc
✓: compound present on MRM-GCMS trace after HyPy
x: compound absent on MRM-GCMS trace after HyPy
See Chart I for sterane structures, sponges are listed in the same order as in Table S4 for specimens of the same species